



UiT The Arctic University of Norway

Faculty of Biosciences, Fisheries and Economics

Department of Arctic and Marine Biology

Spring sea ice algal development in the sub-Arctic Ramfjorden,
northern Norway

Emma Persson

BIO-3950 Master thesis in Biology – May 2020



Frontpage: Ramfjorden, 12th of April 2019. Rowan Romeyn

Acknowledgments

First and foremost, I want to say thank you to my supervisor Rolf Gradinger for giving me this opportunity and for all the knowledge that I have gained from it. Your guidance has made me develop and grow so much in this field. And last but not least, for always making me laugh even when things were feeling tough.

And a huge thanks to my supervisor Ulrike Dietrich for the guidance in this thesis and help during my field work. We had a lot of challenges, but I have learned so much and had a lot of fun in your company.

A big thanks to my supervisor Tobias Vonnahme for great advice and being the expert in R when I needed help. And thank you to both Ulrike and Tobias for sharing your samples and data from Billefjorden with me.

A huge thanks to my classmates in UNIS AB-330, Ecosystems in ice covered waters, for assisting me with my sampling and processing of samples in the field at Van Mijenfjorden. And a special thanks to Janne Søreide for allowing me to sample for my thesis during the field work of the course.

And to Jozef Wiktor for always helping me with identification of species both in person and over email.

I would also like to thank Lucie Goragner. For collaborating with me in the field both in Ramfjorden and in Van Mijenfjorden and for helping each other along the road. And Rose Marie Bank for helping me get started and for a lot of laughter in the process. Thanks to Martial Leroy for helping me with creating maps.

And thank you to my friends at UiT who have helped me in so many ways during this thesis with support, lab work and a lot of fun in between the work.

And last but not least, a huge thank you to my family and friends who have been an unwavering support and always believed in my capacity. It means the world! And to Hassan, for everything.

Abstract

The seasonal development of sea ice algae and bacteria was investigated in Ramfjorden, Norway, from February to April 2019 and compared to data from two Arctic fjords, Van Mijenfjorden and Billefjorden, sampled in April 2019. The sea ice in Ramfjorden was heavily freshwater influenced with bulk salinities ranging from 0.0 to 2.8, similar to those found in freshwater influenced Baltic Sea ice. The low bulk salinities and low brine volume fractions in combination with warm temperatures and low brine salinities resulted in a distinctly different Ramfjorden sea ice environment compared to typical marine high Arctic sea ice systems. One station in Billefjorden, located at the front of a tidewater glacier, was however similar to the sea ice environment in Ramfjorden which indicates that the freshwater input from the glacier had similar effects on the sea ice environment. Ramfjorden had a high snow depth of 10.5 to 52.5 cm during most of the time resulting in reduced light availability for algal growth. The abiotic variables combined resulted in low algal and bacterial abundances, that generally stayed two or more orders of magnitude below those from Arctic sea ice in spring. The algal community in Ramfjorden showed a seasonal succession from almost complete dominance of flagellates at the start of the ice season in February to a higher abundance of diatoms dominated by the centric diatom *Leptocylindrus minimus*. This succession was dependent on the age of the ice and in-ice algal growth and not defined through interactions with the phytoplankton community. Ramfjorden could in future studies be used as a model system to analyse the influence of freshwater run-off on sea ice systems and if its change will have a larger impact on high Arctic systems in the future.

Keywords: Ramfjorden, sub-Arctic fjords seasonality, freshwater influenced fjord, sea ice algae, bacteria.

Abbreviation list

BF – Billefjorden

Chl *a* – Chlorophyll *a*

RF – Ramfjorden

VMF – Van Mijenfjorden

Table of contents

Acknowledgments	1
Abstract	2
Abbreviation list	3
Introduction	5
Ice formation and habitat characteristics	5
Sea ice as a habitat	6
Fjord systems	8
Sample sites	9
Aim of the thesis	11
Material and methods	13
Sampling procedures	13
Chlorophyll <i>a</i> determination	15
Nutrients	15
Bacterial abundance determination by DAPI staining	15
Algal species abundance estimates	16
Statistics	16
Results	18
Physical and chemical variables	18
Snow cover	18
Ice thickness	18
Temperature and salinity	19
Nutrient concentrations	25
Biological variables	28
Chlorophyll <i>a</i>	28
Bacterial abundance	30
Algal abundance	31
Community structure	32
Discussion	36
General outline of the discussion	36
Physical and chemical variables	36
Biological variables	40
Critique of methods	44
Conclusions	45
References	47
Appendix	54

Introduction

Ice formation and habitat characteristics

Sea ice is inhabited by unique sympagic communities occurring in polar and sub-polar areas (Kaartokallio et al. 2016). Ice formation is initiated by the atmospheric temperature decrease with the onset of the winter months. The typical ocean water freezing point is approximately -1.8°C at a salinity of 35 (Staley and Gosink 1999). Sea ice formation characteristics are determined by the condition of the water column and the surrounding environment. When the conditions of the water column and atmosphere are calm, the ice formation and growth rate are mostly dependent on the decrease in temperature (Petrich and Eicken 2016). When the atmosphere cools down and surface water temperature approaches freezing point, ice crystals begin to form and accumulate in a horizontal layer at the surface. With continuing freezing conditions, ice crystals grow vertically (thermodynamic ice growth) and the ice thickness increases over the cold winter months (Arrigo 2014). Such conditions often lead to a relatively smooth ice surface at both the top and at the bottom of the ice.

Ice formation during more turbulent conditions (dynamic ice growth) is affected by wind and therefore also waves in the upper water column (Petrich and Eicken 2016). The ice crystals are then formed in the mixed layer of the water column and a homogeneous surface layer is not created until calmer conditions are reached and the ice crystals accumulate at the surface, called grease ice (Arrigo 2014). The grease ice continues growing with cooling temperatures and will form patches of thicker ice called pancake ice. These pancakes will with time form bigger pancakes while they continue to collide into each other. This process, called the pancake ice cycle, will continue and form a thicker ice sheet that is uneven and rough at both the surface and at the bottom (Lange et al. 1989).

While the ice forms, salt ions are rejected from the solid ice crystals and brine channels, small pockets or tubes, form within the ice with higher salinity and nutrient concentration than the surrounding ice. The salinity in these brine channels is relatively high, reaching salinities above 100 (Gradinger and Bluhm 2018), while the cold ice is formed/growing and a large fraction of the brine will be rejected into the water column in the form of brine drainages (Granskog et al. 2006). The loss of brine will continue as long as the brine volume is above ca. 5% (of the ice volume). But as the brine volume decrease below this, the brine channels becomes isolated from each other and therefore slows down the brine drainages, following the “law of fives” (Golden et al. 1998). This postulates, that ice at a temperature of -5°C and a salinity of 5 has a brine volume of 5% and is permeable while e.g. further cooling makes it

impermeable. The salinity of the brine channels is only determined by the temperature of the ice (Gradinger and Ikävalko 1998). Warmer temperatures increase the size of the channels/pockets and therefore decrease the salinity as the liquid gets diluted, while colder temperatures decrease the size and hence increase the salinity. Brine channel sizes can range from a few micrometres to the centimetre range (Weissenberger et al. 1992; Krembs et al. 2000). Sea ice physical properties within ice floes are often defined by steep gradients in temperature, nutrient availability, salinity, and light (Van Leeuwe et al. 2018). Nutrient concentrations are increasing conservatively with increasing salinities in the brine, as described above, into the sea ice during ice formation and later by exchange with under-ice water into the brine channels. The nutrient concentrations in the ice can therefore vary depending on ice permeability and transport from the sea water below. Nutrients can also be added to the sea ice from the top in the form of precipitation as snow or rain brings nutrients from the atmosphere (Granskog and Kaartokallio 2004). A thick and heavy snow load causes surface flooding by lowering the ice/water interface below sea level (negative freeboard), advecting nutrients from the water column (Sturm and Massom 2016). The light is altered by the ice thickness and snow cover on the ice. Snow has a high albedo and attenuation, and a thick and specifically dry snow cover can therefore drastically decrease the light reaching the organisms living in the ice (Campbell et al. 2018).

Ice can form both in the open ocean, leading to drifting pack ice, and at the coast, forming landfast ice (Thomas et al. 2017). Pack ice formed in the open oceans will be affected by wind, currents and drift (Haas 2016) while landfast ice is connected to the shore throughout the ice season (Gradinger and Bluhm 2018).

Sea ice as a habitat

Sea ice is an important habitat for many species during the ice-covered winter months in seasonal sea ice zones, and year-round in the multiyear ice regions of the Arctic. Organisms such as algae and bacteria are incorporated into the ice by two processes, scavenging and wave-field pumping. For scavenging, cells are harvested by ice crystals as they rise towards the water surface and thereby incorporated into the newly formed ice (Garrison et al. 1989), while wave-field pumping adds organisms into already existing sea ice (Spindler 1994). Primary producers in this habitat are incorporated into the sea ice as it is formed or throughout the ice season through further growth, water exchange between the water column and brine channels, and/or exchange between ice floes (Olsen et al. 2017). The sea ice offers protection from the rough and often deeply mixed water column and provides microhabitats unreachable

for larger pelagic herbi- and carnivores such as larger copepods or euphausiids. This habitat also comes with extreme challenges for the organisms. Two of the main stressors that all ice organisms must be able to adapt/acclimate to are the often low temperatures and high salinities in the brine channels, that both can quickly change (Van Leeuwe et al. 2018). A steep gradient can frequently be seen in these two variables and the bottom sections of the ice are often the least demanding/stressful layers in the sea ice for the ice biota leading to highest abundances there, specifically in the Arctic (Arrigo 2016). The sea-ice – ocean interface has a high abundance, specifically of sea ice algae, as conditions are similar to those of the water column and nutrient availability is higher (Cota and Smith 1991). These sea ice algae communities are often dominated by diatoms with unusually high acclimation and adaption capabilities to the extremely variable sea ice physical and chemical environment (Kooistra et al. 2007). Pennate diatoms contribute on average up to 60% of the relative algae abundance across the Arctic with the colony forming pennate species *Nitzschia frigida* and *Fragilariopsis cylindrus* dominating this group (Hop et al. 2020). While diatoms are in general the dominating group in sea ice during the spring in both Arctic and sub-Arctic areas, small flagellates can dominate the ice in wintertime in e.g. the northern Baltic Sea (Piparinen et al. 2010).

High latitude primary producers in general, and specifically in sea ice, face light limitation during the polar night and in early spring. They are dependent on sunlight for photosynthesis and the abundance is therefore often lowest during this period (Townsend 2012). Algae have developed different strategies to survive this period when some enter dormancy while others build up energy reserves during the productive months (Berge et al. 2015; Johnsen et al. 2020). The sea ice algal community starts to grow at a higher rate than phytoplankton when the sun returns in spring if the above listed physical/chemical conditions are favourable. Snow conditions have a high influence, as dry snow reflects up to 90% of the incoming irradiance back to the atmosphere (albedo), reducing the growth of the sea ice algae community (Leu et al. 2015). Pelagic phytoplankton spring blooms, specifically in seasonal ice zones often reach much higher total biomass and production than those of sea ice algae but ice algal blooms are still of great importance since they occur weeks to months before the larger pelagic blooms and therefore create an important food source for organisms both in the pelagic and benthic communities (Gradinger and Bluhm 2018). The phytoplankton community in the water column are often dominated by small mixotrophic and heterotrophic flagellate species in wintertime when light levels are low, but a succession towards diatoms species towards spring

can often be seen with centric and pennate genera *Thalassiosira*, *Chaetoceros* and *Fragilariopsis* dominating (Johnsen et al. 2020).

Sea ice bacteria have been recorded in high abundances in many field studies both in the Arctic and sub-Arctic (e.g. Haecky and Andersson, 1999; Deming and Collins, 2016). It is thought that bacteria are incorporated into the sea ice with help of carrier algae, and the abundance of bacteria at this point is determined by the abundance of the algae (Grossmann and Gleitz 1993). While ice bacteria are well adapted to cold temperatures, a period of reduced metabolic activity occurs after incorporation, followed by faster growth (Grossmann and Dieckmann 1994). In general, a tight coupling between sea ice algae and bacteria can often be seen in the sea ice as bacteria are dependent on organic carbon which is produced by algae from inorganic carbon, CO₂ (Seuthe et al. 2018). An increase in algal biomass therefore also often results in an increase of bacterial biomass and/or productivity.

Fjord systems

Fjords are defined as deep estuaries that have been (or currently are) shaped by land-based glacial ice (Syvitski et al. 1987). They are located in both hemispheres in polar, subpolar, and temperate climate regimes. A fjord belt in each hemisphere can be found north of 43°N and south of 42°S (Syvitski et al. 1987). Many fjord basins are separated from the coastal water by a sill, which is a barrier of sediments left from the glacial retreat, that restricts the exchange of water between inner parts of the fjords and the open ocean (Howe et al. 2010). Some fjords are divided into different basins by additional sills. The different basins can show different characteristics in water masses depending on the sill depth. A shallow sill depth allows little water exchange between basins, while a deep sill depth allows larger water volumes to move between the basins including also deeper water layers. The circulation in a fjord can therefore be different depending on number of sills and sill depths, but a clear salinity driven stratification can usually be seen, related to freshwater run from land and higher salinity water input from the open ocean or outer coast. Many fjords have three distinct layers where the surface layer has a low salinity, an intermediate layer with intermediate salinities, and a bottom layer with highest salinity (Skardhamar and Svendsen 2010). The surface layer is influenced by land and glacial run-off, the intermediate layer from advected masses external to the fjord and the bottom layer additionally from high salinity sources such as brine drainage and intensely cooled water (Cottier et al. 2010). The two top layers are often transporting the less dense, lower salinity waters outwards towards the fjord mouth while the more dense, higher salinity water from the outer coast creates an inflow in the deeper layer as a

compensation for the surface outflow (Syvitski et al. 1987). This stratification structure occurs mainly during a few months in the summer, while cooling in the colder months can cause a deep mixing of the water masses (Skardhamar and Svendsen 2010).

Sample sites

Ramfjorden

The sub-Arctic Ramfjorden (Figure 1) was the main study site for this thesis. It is located in Tromsø municipality in northern Norway. The fjord is 13 km long and has an outlet to Balsfjorden. It has its deepest point close to Holma (136 m) and its shallowest point close to Storsteinbukta (6 m) with an average depth of 44 m (Noji et al. 1993). Ramfjorden has a number of river outlets connected to the fjord with the largest river at the innermost point, Sørbotnelva. The fjord is typically partially covered by fast ice each year from January/February to April.

Van Mijenfjorden

Van Mijenfjorden (Figure 2) is a two-silled fjord located on the west coast of Svalbard. It is a 50 km long fjord with a mean width of 10 km (Skardhamar and Svendsen 2010). The fjord's mouth is almost completely blocked by the island Akseløya and the exchange of water between the ocean and the fjord takes place in the narrow sounds on either side of the island (Fer and Widell 2007). The fjord is divided into two basins separated by a sill of 45 m where the outer basin is 115 m deep and the inner 74 m deep (Skardhamar and Svendsen 2010). Two glaciers calve in the fjord, one located at the innermost part of the fjord (Paulabreen) and one near the fjord mouth (Fritjovbreen) (Skardhamar and Svendsen 2010). The high Arctic Van Mijenfjorden has a longer fast ice covered season than Ramfjorden and becomes ice covered in December/January, and ice melt starts in the beginning of the summer around June/early July (Høyland 2009).

Billefjorden

Billefjorden (Figure 3) is a branch of Isfjorden on the west coast of Svalbard. The 30 km long fjord is separated from Isfjorden by a 50 m deep sill at the fjord's mouth (Szczuciński et al. 2009). The tidewater glacier Nordenskiöldbreen has its terminus in Adolfbukta, a branch of Billefjorden. The main basin has an average depth of 160 m (Nilsen et al. 2008). Billefjorden,

like Van Mijenfjorden, has a longer fast ice covered period than Ramfjorden and is usually only ice free from July to late November (Szcuciński et al. 2009).

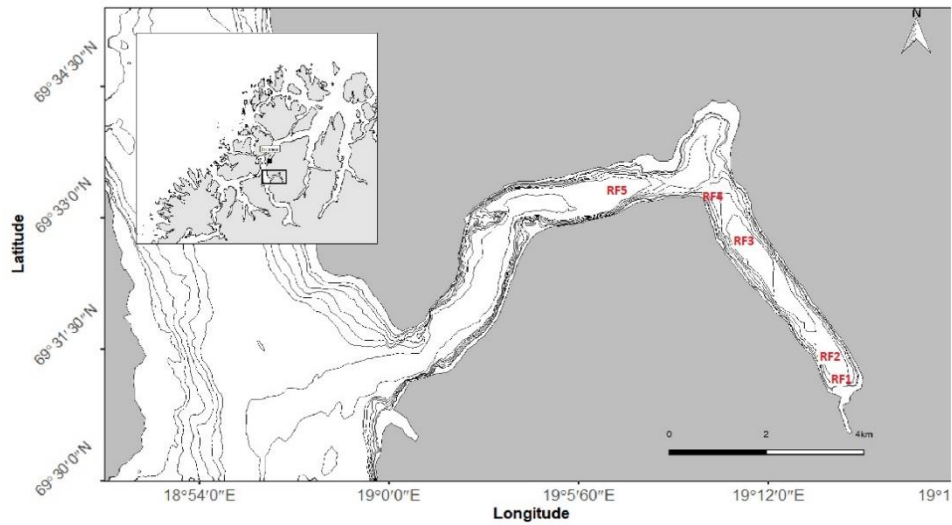


Figure 1. Station map of Ramfjorden (Kartverket).

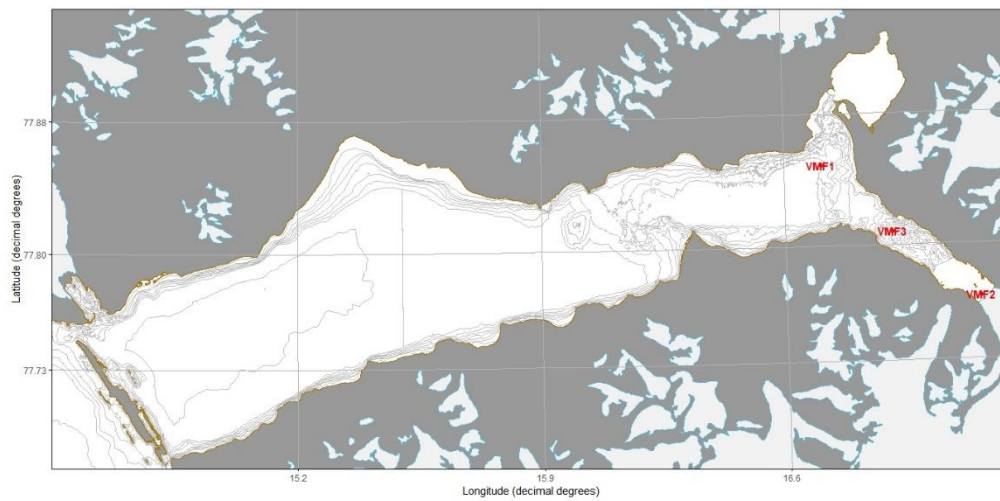


Figure 2. Station map of Van Mijenfjorden (Norwegian Polar Institute).

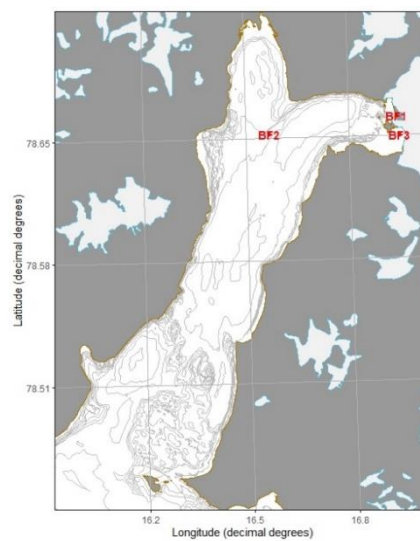


Figure 3. Station map of Billefjorden (Norwegian Polar Institute).

Aim of the thesis

The physical, chemical, and biological properties of sea ice can vary greatly depending on e.g., location, season, changes in local environment and ice/ocean interactions. High Arctic fjords may be covered by sea ice in the winter months and experience extreme light regime with polar nights and midnight sun. On the other hand, fjords located on lower latitudes will often have shorter winter and sea ice cover periods, a more stable light regime, and as in Saroma lagoon, Japan, and the Baltic Sea, a heavy influence by freshwater from river run-off (Robineau et al. 1997; Granskog et al. 2006). Another freshwater source that can influence the fjord system in the high Arctic are tidewater glaciers, as seen in e.g. southwestern Greenland (Krawczyk et al. 2015). These differences will cause differences in the physical and chemical characteristics of the ice, which in turn will impact the biomass and diversity of organism community living in the sea ice. This study tested for the first time if the sub-Arctic Ramfjorden sea ice biology is comparable to the marine influenced high Arctic fjord systems or to the sub-Arctic more freshwater influenced systems like the Baltic Sea or Saroma Lagoon. The seasonal study established in this thesis covered the onset of the spring period and included measurements of sea ice physical, chemical and biological variables, allowing to address the following main research question:

- Does Ramfjorden sea ice provide a typical sea ice environment for biota as seen in other Arctic and/or sub-Arctic systems?

The following hypotheses were addressed:

- Ramfjorden sea ice differs in its physical and chemical properties from high Arctic fjord sea ice due to the different growth conditions.
- Ramfjorden sea ice communities do not follow the typical biomass vertical distribution patterns observed in high Arctic systems due to different environmental conditions.
- Ramfjorden ice algal biomass will be lower than in high Arctic sea ice due to reduced inhabitable space due to ice formation in a brackish water environment.
- Species composition of ice algae in Ramfjorden will be different to those of high Arctic ice algal communities.
- Biomass estimates in Ramfjorden sea ice will exceed phytoplankton biomass during early spring.

- Ramfjorden can be used as a model system to study the influence of freshwater on sub-Arctic ice systems.
- Tidewater glaciers influenced high Arctic sea ice systems may have similar sea ice structures, communities and biomass as the river and meltwater influenced sub-Arctic Ramfjorden.

Material and methods

Sampling procedures

Monthly sampling was conducted in Ramfjorden (Figure 1), Norway from February to April 2019 (Table 1). For comparison, high Arctic samples were obtained from fast ice areas in Van Mijenfjorden (Figure 2) and Billefjorden (Figure 3) in Svalbard in April 2019. At each site, ice cores and water samples were taken on each sampling date for subsequent analysis in the lab. The sampling itself was conducted as follows. First, snow depth was measured with a ruler. Following snow removal, ice cores were collected using a Mark II 9 cm inner diameter ice corer (Kovacs Enterprise, Roseburg, OR, USA). One ice core was used to measure the ice core temperature by inserting a temperature probe (TD20, VWR, USA) into 3 mm diameter drilled holes every two to ten centimetres along the complete vertical profile. Additional ice cores were sub-sectioned with a saw immediately after coring into the following sections (distances given from ice-water interface): bottom 0-3 cm, 3-10 cm, and thereafter into 10 cm sections in Ramfjorden, and 20 cm sections in Van Mijenfjorden and Billefjorden until the top of the ice core. The sub-sections were put into Whirl-Pak bags and stored in a cooler box to protect them from melting and light exposure. Water from one meter below the ice was sampled with a water sampler (Ruttner sampler, 2 L capacity, HYDRO-BIOS, Germany). The water was transferred into acid-washed plastic containers wrapped in black foil to avoid light exposure.

The ice core sections were treated in two different groups in the lab. The first set of ice core sections was used for measuring Chlorophyll *a* (Chl *a*), algal cell abundance and identification, and bacterial abundance and were melted individually with the addition of 0.2 µm sterile filtered sea water (approximate sea water salinity of 34, 50 ml addition per cm of ice section thickness in RF and 100 ml addition per cm of ice section thickness in VMF and BF) to reduce the effect of osmotic shock. The second set of sections was individually directly melted without the addition of sterile filtered water and used for determination of ice bulk salinity and nutrient concentrations. During melting all samples were stored in the dark at 4°C. Salinity of the directly melted ice core sections was measured with a conductivity probe (YSI Pro 30, YSI, USA) after complete ice melt.

Table 1. Overview of sampling stations.

Station	Site	Date	Latitude (deg. N)	Longitude (deg. E)	Ice thickness (cm)	Snow depth (cm)
RF1	Ramfjorden	7/2/19	69.519	19.236	25.0	12.0
RF2	Ramfjorden	7/2/19	69.523	19.230	36.0	15.0
RF3	Ramfjorden	8/2/19	69.545	19.185	36.0	10.0
RF1	Ramfjorden	15/3/19	69.519	19.236	45.0	28.0
RF2	Ramfjorden	15/3/19	69.523	19.230	36.0	20.5
RF3	Ramfjorden	14/3/19	69.545	19.185	39.0	24.5
RF4	Ramfjorden	19/3/19	69.555	19.167	17.0	10.5
RF5	Ramfjorden	19/3/19	69.555	19.120	17.0	13.5
RF1	Ramfjorden	2/4/19	69.519	19.236	45.0	52.5
RF2	Ramfjorden	3/4/19	69.523	19.230	48.0	24.5
RF3	Ramfjorden	2/4/19	69.545	19.185	43.0	44.5
VMF1	Van Mijenfjorden	26/4/19	77.849	16.706	75.0	8.0
VMF2	Van Mijenfjorden	28/4/19	77.768	17.155	86.0	15.0
VMF3	Van Mijenfjorden	30/4/19	77.808	16.907	83.0	13.5
BF1	Billefjorden	27/4/19	78.661	16.938	92.0	6.0
BF2	Billefjorden	28/4/19	78.652	16.566	79.0	10.0
BF3	Billefjorden	25/4/19	78.650	16.945	128.0	3.0

Chlorophyll *a* determination

Water and melted ice samples were filtered through GF/F filters in triplicates for each ice section/water depth and station. The filters were put into 15 ml Falcon tubes wrapped with aluminium foil and stored in the freezer (-20 °C) until further processing. For pigment extraction, 5 ml of 96% ethanol was added to each filter and stored in the fridge (4°C) for 24 hours. 30 minutes prior to analysis, samples were taken out of the fridge to reach room temperature. Samples were mixed using a Vortex and Chl *a* fluorescence was quantified with a Turner Trilogy fluorometer using standard techniques (Turner Designs 2019). A blank reading with pure 96% ethanol was determined at the start of each Chl *a* measurement. After the initial read of the sample, two drops of 5% HCl were added to the cuvette which was then placed back into the fluorometer to measure the fluorescence in the acidified sample. The calculations of Chl *a* and pheophytin concentrations were made using the Chl *a* acidification technique module produced by Turner (USA).

Nutrients

Inorganic nutrient samples were filtered through a 0.2 µm syringe filter (polyethersulfone membrane) prior to freezing (-20 °C) to remove cells that would burst during melting. The filtered samples (50 ml) were stored in acid-washed and sterile distilled water (MQ) washed Falcon tubes. Prior to analysis, the samples were taken out of the freezer, thawed at room temperature, and transferred to plastic tubes. Analyses of the concentrations of nitrate (QuAatro manuals: Method No. Q-068-05 Rev. 12), nitrite (Method No. Q-068-05 Rev. 12), silicate (Method No. Q-066-05 Rev. 5), and phosphate (Method No. Q-064-05 Rev. 8) were conducted colorimetrically with a nutrient autoanalyzer (QuAatro, SEAL Analytical, Germany) in triplicate using the instrument specific techniques listed for each nutrient.

Bacterial abundance determination by DAPI staining

A Falcon tube was filled with 1.3 ml of 37% formaldehyde (CH₂O) and 23.7 ml of sample water (2 % final concentration). The samples were stored in a fridge (4 °C) for 24-48 hours and filtered onto 0.2 µm polycarbonate filters (Whatman) supported by a GF/F filter underneath to ensure even distribution of the cells. The polycarbonate filter was then washed in 96% ethanol and sterile distilled water (MQ) before being placed in a petri dish with the lid slightly open to make the filter dry before being stored in the freezer (-20 °C).

The fluorescent dye DAPI (4,6-diamidino-2-phenylindole) is light sensitive and therefore the following steps were done in little light or in the dark (Porter and Feig 1980). The sample filters were wiped in 20 µl of DAPI solution (1 µg/ml) and another 10 µl was added on top of

the filter. After 5 minutes of incubation at room temperature, the filters were washed in sterile distilled water (MQ) and 96% ethanol and left to dry in a petri dish.

After DAPI staining, a drop of Citifluor-Vectashield™ solution (ratio: 4:1) was added to a microscope slide before the filter was placed on top faced up. Another drop of Citifluor™-Vectashield™ solution was added to the top and a cover slip was put on top, and slight pressure was added to flatten the filter out, remove air bubbles and to spread the medium along the slide. The filter was then stored in the freezer (-20 °C) to intensify the fluorescence signal for at least one hour before cell counting. The bacterial cells were counted using an epifluorescence microscope (Leica DM LB2, Leica Microsystems, Germany) under UV light excitation at 100x magnification using non-fluorescent immersion oil. Cells were counted in grids or parts of a grid until a minimum number of 200 bacteria were counted within at least 10 grids.

Algal species abundance estimates

100 ml of the melted ice or water sample were fixed with neutral Lugol (1-2% final concentration) and stored in a brown glass flask. 10-50 ml of the sample were settled in specific chambers using the Utermöhl method for a minimum of 24 h (Utermöhl 1958). Counting and identification of algal cells was conducted under an inverted microscope (Zeiss Primovert, Carl Zeiss AG, Germany), and at least 400 cells were counted along transects or fields of view. General taxonomic literature on phytoplankton and sea ice algae (e.g. Tomas, 1997; Throndsen et al. 2007) and confirmation by Jozef Wiktor (Institute of Oceanology, Polish Academy of Science, Sopot, Poland) were used to identify organisms to the lowest taxonomic level possible.

All species names were checked for validity using the online database www.marinespecies.org on 2020-04-14.

Statistics

An unpaired t-test ($\alpha=0.05$) was used to test for significant differences in means of different variables using R. Normality was tested beforehand by using Shapiro-Wilk normality test.

A multivariate statistical analysis was done with the vegan package (Oksanen et al. 2007) in R (R Core Team 2020). Non-metric multidimensional scaling (NMDS) was used to understand the dissimilarities between stations with stations being more similar to each being closer in the resulting two dimensional plot, which was created using the metaMDS function based on Bray-Curtis dissimilarities. The calculated stress level for the plot can be used as an indicator

how well the two-dimensional plot represents the true distances between stations, and the stress value should be – as a rule of thumb - below 0.20.

The maps were created in Rstudio. The Ramfjorden map was created using geospatial data from Kartverket (2018) while the Svalbard maps were created using the PlotSvalbard package (Vihtakari 2020) with maps from the Norwegian Polar Institute (NPI 2017) and bathymetry files from Kartverket (2015).

Results

The following section outlines first the physical/chemical and then the biological results from the various stations. Note that mostly only a subset of typical results is displayed in the figures in this section, while additional data set for other stations can be found in the indicated appendices.

Physical and chemical variables

Snow cover

The snow depth increased at all three stations in Ramfjorden from February to April (Figure 4a). The largest increase occurred at the innermost station (RF1) with an increase from 12.0 cm in February to 52.5 cm in April. RF1, RF2 and RF3 had similar snow depths in February and March with a maximum of 7.5 cm difference while in April the difference between RF1 and RF2 was 28.0 cm and between RF2 and RF3 20.0 cm. RF4 and RF5, which were only sampled in March as the ice had formed later in the outer fjord, had a thinner snow depth compared to RF1, RF2 and RF3.

The Svalbard stations in Van Mijenfjorden and Billefjorden had a very homogenous snow cover at all stations with VMF stations ranging from 8.0 cm to 15.0 cm and BF stations from 3.0 cm to 10.0 cm (Figure 4a).

Van Mijenfjorden and Billefjorden had a significantly lower snow depth ($p < 0.05$ each) than the sea ice in Ramfjorden in April with the largest difference between RF1 and VMF1 (44.5 cm) for Van Mijenfjorden and RF1 and BF3 (49.5 cm) for Billefjorden.

Ice thickness

The ice thickness in Ramfjorden increased at all stations by 7.0-20.0 cm from February to April. The largest increase occurred at the innermost station RF1 in March (20.0 cm) while RF2 and RF3 had largest increases in April (12.0 cm and 4.0 cm). The relatively newly formed ice at RF4 and RF5 had the thinnest ice cover (Figure 4b).

At the stations at Van Mijenfjorden (Figure 4b) ice thickness ranged from 75.0 cm (VMF1) to 86.0 cm (VMF2). In Billefjorden, ice was thicker with values between 79.0 cm (BF2) and 128.0 cm (BF3, glacier front).

Overall, the April ice thickness was significantly thinner ($p < 0.05$ each) in Ramfjorden versus the Svalbard fjords with the largest difference between RF3 and BF3 (85 cm).

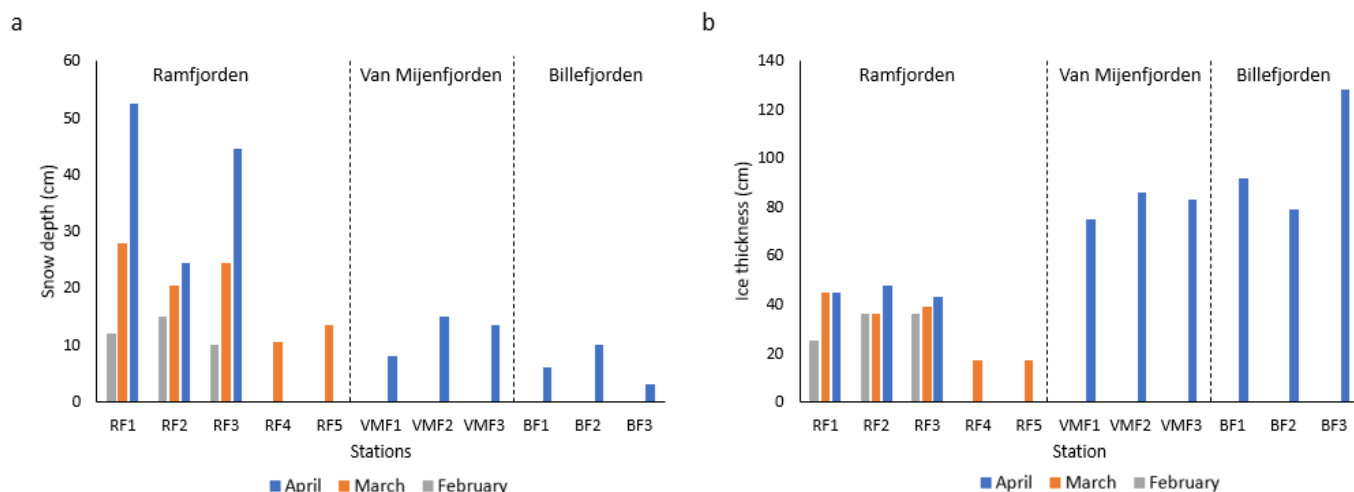


Figure 4. a: Snow depth at all sampled stations, b: Ice thickness at all sampled stations.

Temperature and salinity

The temperatures in the Ramfjorden ice cores ranged from $-0.3\text{ }^{\circ}\text{C}$ to $-3.3\text{ }^{\circ}\text{C}$ in February (Figure 5, Appendix A for RF2). All stations showed similar vertical gradients with highest temperatures at the bottom of the ice core and decreasing temperatures further up the core. The outermost station RF3 had the lowest mean temperature ($-2.3\text{ }^{\circ}\text{C}$, SD: $0.7\text{ }^{\circ}\text{C}$, $n=8$) and the innermost station RF1 had the highest mean temperature ($-0.6\text{ }^{\circ}\text{C}$, SD: $0.2\text{ }^{\circ}\text{C}$, $n=5$). The ice temperatures increased in March at all stations (RF1-5) with temperatures being between $-0.1\text{ }^{\circ}\text{C}$ to $-1.0\text{ }^{\circ}\text{C}$ (Figure 5, Appendix A). Warming continued in April, when temperatures ranged from $0.0\text{ }^{\circ}\text{C}$ to $-0.3\text{ }^{\circ}\text{C}$ at RF1-3.

In Svalbard, the ice temperatures in Van Mijenfjorden ranged from $-0.3\text{ }^{\circ}\text{C}$ to $-2.6\text{ }^{\circ}\text{C}$. The lowest mean temperature was found at the outermost station VMF1 ($-1.9\text{ }^{\circ}\text{C}$, SD: $0.1\text{ }^{\circ}\text{C}$, $n=11$, Figure 5), and the highest at VMF2 ($-1.1\text{ }^{\circ}\text{C}$, SD: $0.3\text{ }^{\circ}\text{C}$, $n=11$, Appendix A). The ice at VMF1 showed a clear vertical temperature gradient with the highest temperatures in the bottom parts of the ice core and colder temperatures at the top, while gradients were less developed at VMF2 and VMF3.

All three stations in Billefjorden showed similar vertical patterns with decreasing temperatures towards the top part of the ice cores (Figure 5, Appendix A) with an overall range between $-0.4\text{ }^{\circ}\text{C}$ and $-3.2\text{ }^{\circ}\text{C}$.

The April ice cores in Van Mijenfjorden and Billefjorden were significantly colder ($p<0.05$ each) than those from Ramfjorden. Furthermore, all cores in Van Mijenfjorden and Billefjorden showed a strong vertical pattern of decreasing temperatures toward the top parts

of the core while the Ramfjorden cores had relatively stable temperatures throughout the whole core.

The calculated brine salinity – based on the ice temperatures – decreased with time at all stations in Ramfjorden from a mean brine salinity in February of 25.7 (SD: 16.4, n=14) to a mean of 2.5 (SD: 2.1, n=15) in April. An overall vertical gradient with increasing brine salinities towards the top of the ice cores could be seen at all stations during the sampling period (Figure 5, Appendix A). Brine salinities also increased from the innermost station RF1 to the outermost stations RF3 in all months and to RF5 in March. In March for example, RF1 had a significantly lower ($p<0.05$) mean brine salinity of 6.7 (SD: 2.8, n=5) in comparison to RF3 that had a mean brine salinity of 11.8 (SD: 3.4, n=5).

The brine salinities of Van Mijenfjorden sea ice ranged from 12.0 to 47.7. VMF1 showed the clearest vertical pattern with increasing brine salinity towards the top sections of the ice core (Figure 5). While principally the same pattern could be seen at VMF2 and VMF3 (Appendix A), gradients were less clearly developed.

The brine salinity in Billefjorden ranged from 7.4 to 57.3 with consistently increasing brine salinity towards the top sections of the ice cores (Figure 5). BF1 and BF2 had a significantly higher mean brine salinity ($p<0.05$ each) than BF3.

Van Mijenfjorden and BF1-BF2 sea ice had significantly higher mean brine salinities (VMF: mean of 29.4, SD: 8.8, n=19, BF: mean of 47.8, SD: 6.7, n=12) than ice in Ramfjorden (mean of 2.5, SD: 2.1, n:15) in April ($p<0.05$, each) with much clearer vertical gradients. BF3 at the glacier front had on the other hand significantly lower mean brine salinities (mean of 14.6, SD: 8.9, n=8) than BF1 and BF2, as mentioned above, but the brine salinities were still significantly higher than at the Ramfjorden stations ($p<0.05$ each).

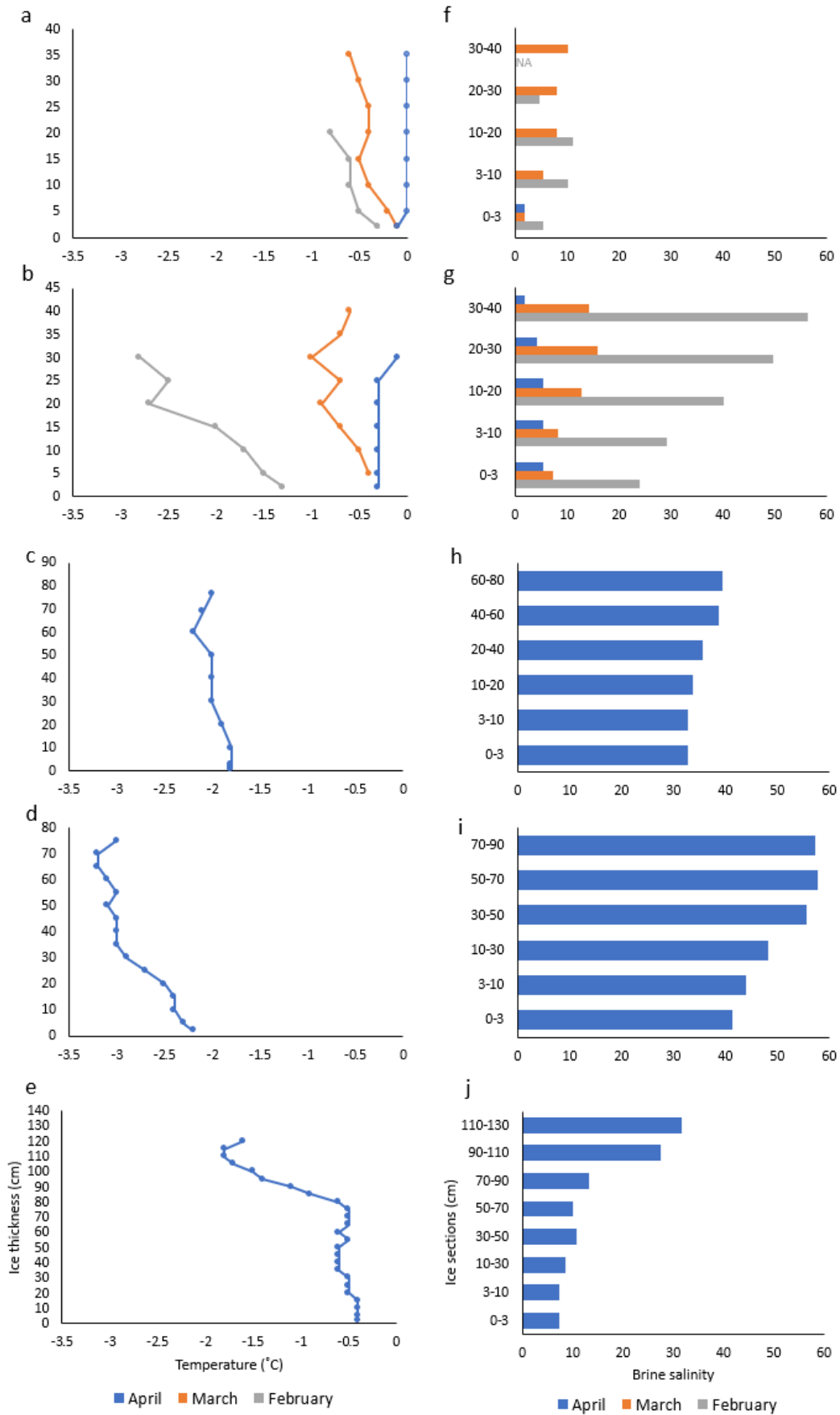


Figure 5. Vertical temperatures (left) and calculated brine salinity gradients (right). a&f: RF1, b&g: RF3, c&h: VMF1, d&i: BF2, e&j: BF3. Data from additional stations can be found in Appendix A.

The bulk salinities in Ramfjorden (Figure 6, Appendix B) decreased over time from a mean bulk salinity of 1.1 (SD: 0.8, n=14) in February to a mean bulk salinity of 0.3 (SD: 0.3, n=15) in April. A vertical pattern with increasing bulk salinity towards the top of the ice cores was overall present at all stations at all three months (Figure 6, Appendix B). A clear gradient with increasing bulk salinities was detected from the innermost station RF1 to the outer stations RF3 (until April) to RF5 (March only).

In Van Mijenfjorden (Figure 6, Appendix B), bulk salinities ranged from 0.7 to 12.0. At VMF1 and VMF3 bulk salinities decreased towards the top of the core. VMF1 had the highest mean bulk salinity (7.7, SD:2.1, n=6) while VMF2 had the lowest mean bulk salinity (4.7, SD:1.8, n=7). The bulk salinity in Billefjorden ranged from 0.0 to 11.2. At BF1 and BF2 bulk salinities decreased towards the top of the cores while BF3 had the highest bulk salinity at the top section of the core. BF2 sea ice had the highest mean bulk salinity (6.1, SD:2.5, n=6) while at BF3 it was lowest (0.5, SD:0.5, n=8).

All stations in Van Mijenfjorden and Billefjorden, with the exception of BF3, had a significantly higher bulk salinity ($p < 0.05$ each) than the Ramfjorden stations in April. All Svalbard stations, except BF3, also showed a vertical pattern of decreasing bulk salinity towards the top sections of the core while this pattern only could be seen at RF1 in Ramfjorden. The mean April bulk salinities in Ramfjorden and at BF3 in Billefjorden were very similar (RF:0.3, SD:0.3, n=15; BF3:0.5, SD:0.5, n=8) and not significantly different ($p > 0.05$).

The brine volume fraction in Ramfjorden was overall increasing from the innermost station RF1 towards the outermost stations RF3 to RF5. A significant difference can be seen for example in mean brine volume ($p < 0.05$) between RF1 (mean:0.3, SD:0.7, n=5) and RF5 (mean:11.3, SD:2.8, n=3) in March. RF1 had overall low brine volumes throughout the time series while a seasonal increase could be seen at RF2 and RF3 (Figure 6, Appendix B). All Ramfjorden stations except RF1 had a vertical gradient with generally increasing brine volume fractions towards the top part of the ice cores.

All stations at Van Mijenfjorden (Figure 6, Appendix B) showed a clear vertical pattern with highest brine volume in the bottom section of the cores and decreasing volumes towards the top. The brine volume in the ice cores ranged from 4.9% to 33.9%.

The brine volume fraction in Billefjorden (Figure 6, Appendix B) at BF1 and BF2 ranged from 2.2% to 16.3% while brine volumes at BF3 was lower and ranged from 0.0% to 8.7%.

The mean brine volume fractions at BF1 (mean:8.9, SD:4.2, n=6) and BF2 (mean: 10.3, SD:3.2, n=6) were significantly ($p<0.05$ each) larger than the mean brine volume at BF3 (mean:3.9, SD:3.0, n=8). BF1 and BF2 generally showed a vertical gradient with decreasing brine volume towards the top sections of the ice core. BF3 showed a C-shaped brine volume curve with largest brine volume in the bottom and top sections.

The stations at Van Mijenfjorden showed significantly larger brine volumes ($p<0.05$, each) compared to Billefjorden and Ramfjorden in April. A clear vertical gradient could be seen at all the stations in Van Mijenfjorden and also at BF2, where the brine volume was largest at the bottom sections of the ice cores and decreased towards the top. RF2 was the only station at Ramfjorden with a vertical gradient in April, but the brine volume was smallest at the bottom section in this case and increased towards the top of the core.

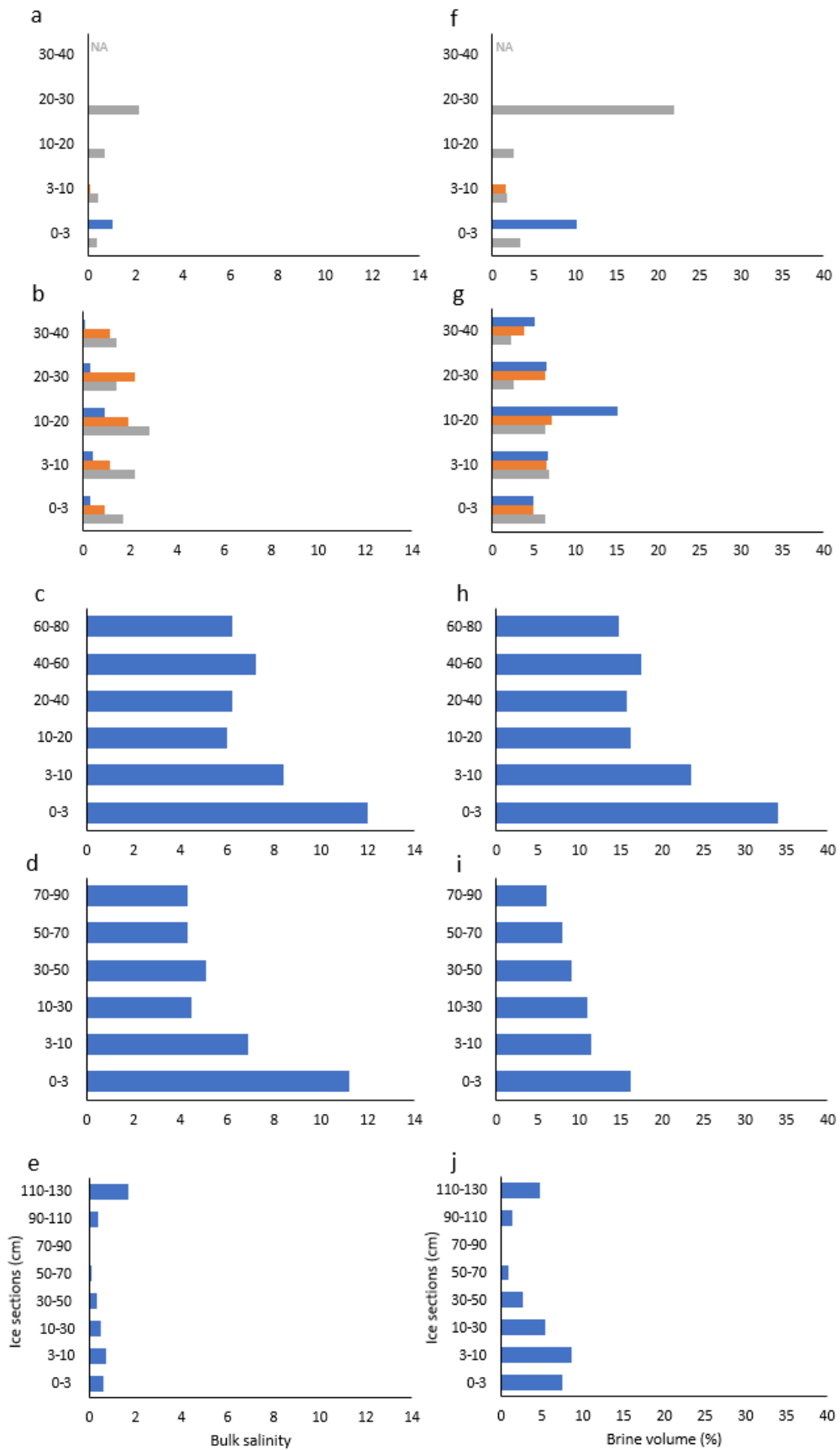


Figure 6. Vertical gradients of ice bulk salinity (left) and calculated brine volume fraction (right). a&f: RF1, b&g: RF3, c&h: VMF1, d&i: BF2, e&j: BF3. Data from additional stations can be found in Appendix B.

Nutrient concentrations

A clear increasing gradient of silicate concentrations from the innermost station RF1 to the outermost stations RF3 to RF5 was found in Ramfjorden (Figure 7, Appendix C). The silicate concentrations in February were higher inside the ice compared to the water column for most samples with ice values of 0.7 to 7.1 $\mu\text{mol/L}$ and water data between 0.3 and 1.8 $\mu\text{mol/L}$. Higher concentrations were found in the top part of the ice compared to the ice interior and bottom. The difference between ice and water changed over time with increasing silicate concentrations in the water column while it generally decreased in the ice cores in March and April. The water column in March had a range of 5.5-11.5 $\mu\text{mol/L}$ exceeding the ice data that ranged from 0.1 $\mu\text{mol/L}$ to 10.8 $\mu\text{mol/L}$. In April, the water column concentrations of 4.8 to 14.3 $\mu\text{mol/L}$ still exceeded the sea ice values, which ranged from 0.1 $\mu\text{mol/L}$ to 4.1 $\mu\text{mol/L}$. All stations except RF1 showed a tendency of having the lowest concentration in the bottom section of the ice (0-3 cm) and increasing concentrations towards the top of the ice core in all months with the biggest relative difference (factor of 2.4) for station RF5 in March.

The sea ice at VMF1 (range: 0.2-0.4 $\mu\text{mol/L}$) and VMF3 (range: 0.2-0.2 $\mu\text{mol/L}$) had significantly lower silicate concentrations ($p < 0.05$ each) (Figure 7, Appendix C) compared to VMF2 (range: 0.6-2.2 $\mu\text{mol/L}$). The water column concentrations ranged from 1.6 $\mu\text{mol/L}$ to 3.5 $\mu\text{mol/L}$ with the highest values found at VMF1.

The water column in Billefjorden had higher silicate concentrations (range: 1.6-3.3 $\mu\text{mol/L}$) than the ice cores with the exception of the 30-50 cm section at BF2. BF3 (range: 0.4-3.2 $\mu\text{mol/L}$) had overall higher concentrations compared to BF1 (0.1-0.4 $\mu\text{mol/L}$) and BF2 (0.1-0.2 $\mu\text{mol/L}$).

Van Mijenfjorden and Billefjorden stations showed lower but not significantly different silicate concentrations ($p > 0.05$) in the water column compared to Ramfjorden in April. Ramfjorden generally had a vertical gradient with values increasing towards the top of the ice cores while this was not seen that clearly in Van Mijenfjorden and Billefjorden.

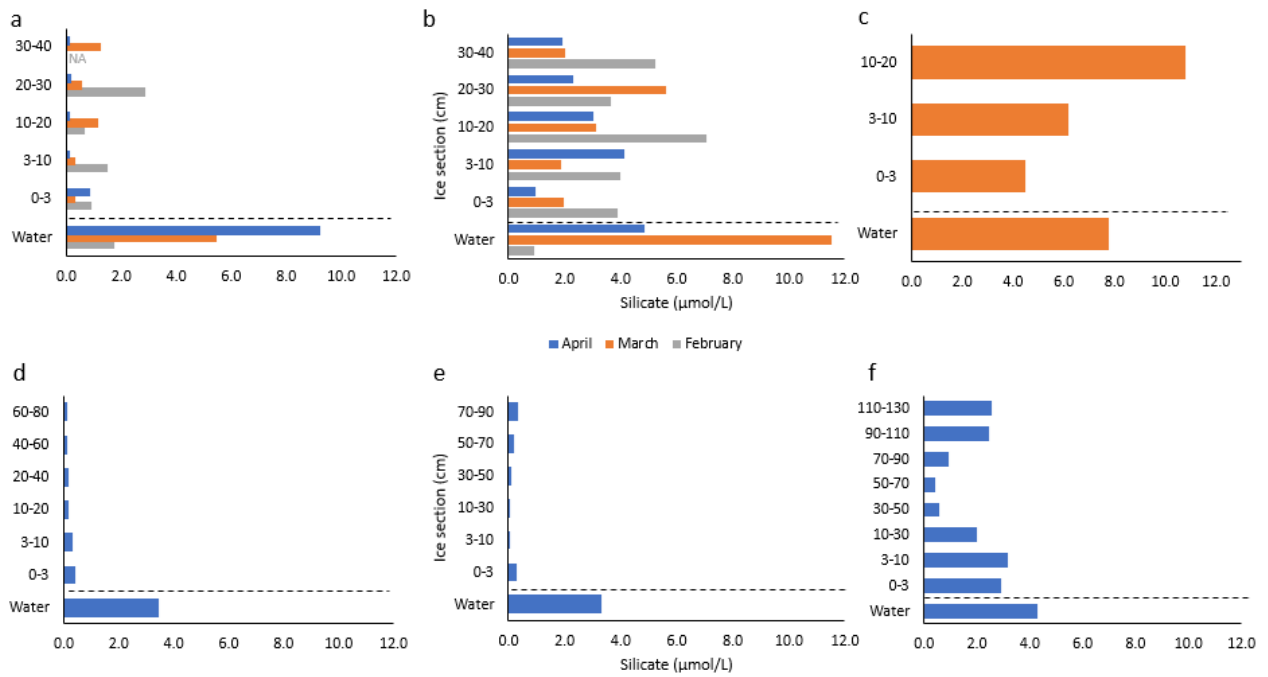


Figure 7. Silicate concentrations in the water column and in the ice core sections. a: RF1, b: RF3, c: RF5, d: VMF1, e: BF2, f: BF3. Data from additional stations can be found in Appendix C.

Nitrate concentrations in Ramfjorden generally decreased from the innermost station RF1 to the outermost station RF3 in February while this gradient reversed in direction in April (Figure 8, Appendix D). Ramfjorden sea ice values were generally lower than the water sample nitrate concentrations in February (sea ice: 0.5-2.9 µmol/L , water: 1.5-5.1 µmol/L) and March (sea ice: 0.5-3.4 µmol/L , water: 4.4-7.6 µmol/L) while the ice cores values exceeded water concentrations at RF2 (sea ice: 0.7-7-1 µmol/L, water: 3.5 µmol/L) and RF3 (sea ice: 4.7-6.5 µmol/L , water: 2.2 µmol/L) in April. A vertical gradient could generally be seen throughout the time series with increasing concentrations of nitrate towards the top of the cores.

Both VMF1 and VMF2 showed a C-shaped pattern in ice nitrate concentrations, which were highest in the bottom and top section (Figure 8, Appendix D). The concentration in the ice had a range of 0.3-4.5 µmol/L while the water column nitrate concentration was lower and ranged between 0.2 to 0.5 µmol/L.

At all stations in Billefjorden, water column nitrate concentrations were exceeding ice data with a range from 3.3 to 7.6 µmol/L. BF1 showed the same C-shaped pattern as VMF1 and VMF2 with the highest concentrations in the bottom and top sections (Figure 8, Appendix D). BF3 had overall higher concentrations of nitrate (range: 0.4-3.3 µmol/L) in the ice core than BF1 (range: 0.1-1.5 µmol/L) and BF2 (range: 0.2-1.0 µmol/L).

In April most stations (except for RF2, RF3 and VMF2) had the highest concentration of nitrate in the water column. All sea ice cores in Van Mijenfjorden had the highest concentrations in the top part of the core in contrast to the Ramfjorden samples where this section had the lowest concentrations.

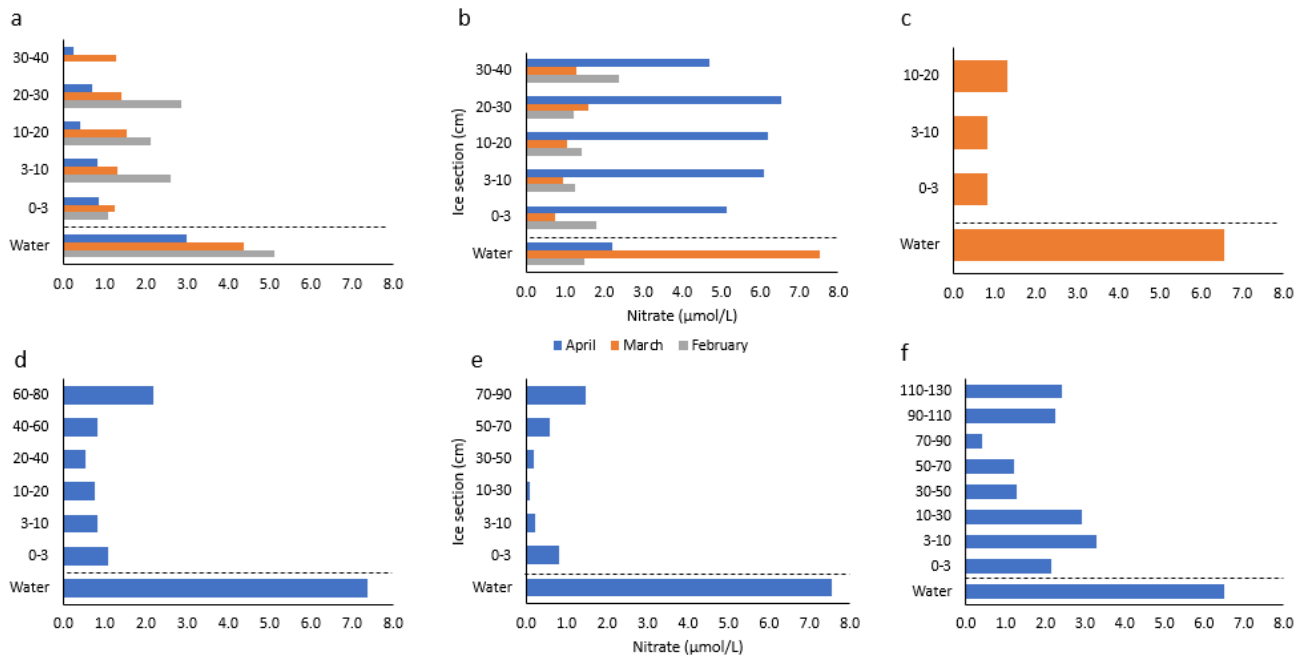


Figure 8. Nitrate concentrations in the water column and in the ice core sections. a: RF1, b: RF3, c: RF5, d: VMF1, e: BF2, f: BF3. Data from additional stations can be found in Appendix D.

Phosphate concentrations increased in Ramfjorden from the innermost station RF1 to the outer station RF3 (Figure 9, Appendix E). Although concentrations were very low, water column phosphate concentrations at all three stations were higher in February (range: 0.0-0.1 µmol/L) compared to the ice cores (range: 0.0-0.1 µmol/L). The phosphate concentration in the water column increased in March at RF1 and RF2 while it decreased at RF3. The water column still had the higher concentrations at all stations (range: 0.0-0.5 µmol/L) compared to the ice cores (<0.1 µmol/L) with the exception of RF4 where the 3-10 cm section had a slightly higher concentration than the water sample. April concentrations showed the same pattern as the previous months with the highest concentrations in the water column (range: 0.1-0.2 µmol/L) compared to the ice cores (range: 0.0-0.1 µmol/L).

Van Mijenfjorden (Figure 9, Appendix E) had the highest concentrations of phosphate in the water column (range: 0.2-0.5 µmol/L). Ice values ranged from 0.0 µmol/L to 0.2 µmol/L. VMF1 had the highest concentration in the bottom section (0-3 cm) and decreasing concentrations towards the top part of the core while VMF2 and VM3 had more homogenous concentrations throughout the cores.

Billefjorden (Figure 9, Appendix E) showed highest phosphate concentrations in the bottom section (0-3 cm) at BF1 and BF2 while BF3 had the highest concentrations in the water column. The water column values in Billefjorden ranged from 0.3 $\mu\text{mol/L}$ to 0.5 $\mu\text{mol/L}$ and the ice cores from 0.0 $\mu\text{mol/L}$ to 1.3 $\mu\text{mol/L}$.

Both Van Mijenfjorden and Billefjorden showed higher concentrations of phosphate in the water column compared to Ramfjorden in April (RF-BF: $p < 0.05$, RF-VMF: > 0.05). VMF1, BF1 and BF2 had higher concentrations in the bottom section (0-3 cm) while the other stations in April had a more homogenous phosphate concentration throughout the core.

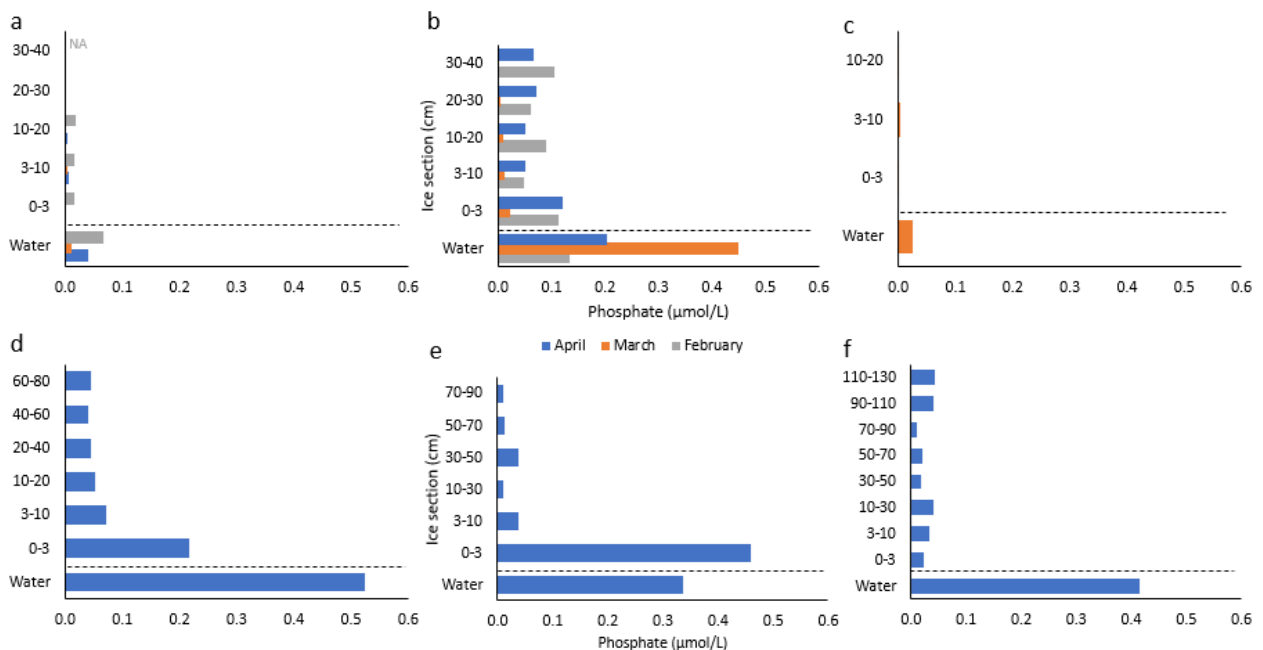


Figure 9. Phosphate concentrations in the water column and in the ice core sections. a: RF1, b: RF3, c: RF5, d: VMF1, e: BF2, f: BF3. Data from additional stations can be found in Appendix E.

Biological variables

Chlorophyll *a*

Chl *a* concentrations were non-detectable or very low in February at RF1-3 in Ramfjorden both in the water column and the ice cores with concentrations in a range of 0.0-0.2 $\mu\text{g/L}$ (Figure 10, Appendix F). Chl *a* concentrations at all stations increased in March with water values exceeding ice data all station (except RF3) by a factor of 1.8 to 3.1. RF3-5 had the highest concentrations in the ice cores in the lowermost 3 cm of the ice cores (range: 0.6-0.7 $\mu\text{g/L}$) with decreasing concentrations further up in the core. For most stations, ice Chl *a* concentrations decreased towards April. The water Chl *a* concentrations increased at RF2 and RF3 compared to March while it decreased at RF1 with overall concentration of 0.4 $\mu\text{g/L}$ to 1.1 $\mu\text{g/L}$.

All three stations in Van Mijenfjorden showed distinct ice bottom maxima with the highest Chl *a* concentration in the 0-3 cm section with the highest value at VMF1 (32.7 µg/L) and lowest at VMF3 (4.2 µg/L) (Figure 10, Appendix F). The phytoplankton Chl *a* concentrations at all three stations were significantly lower ($p < 0.05$ each; range: 0.2-0.5 µg/L) than the related bottom ice values by factors of 6 to 733.

All Billefjorden stations showed the same pattern as the Van Mijenfjorden stations with highest values of Chl *a* concentrations in the 0-3 cm section (Figure 10, Appendix F) with maximum values at BF1 and BF2 while the bottom maximum at BF3 was much lower with 0.7 µg Chl *a*/L. The water column values at BF1 and BF2 were below 2 µg/L. Surprisingly, the relatively high BF3 water concentration (4.3 µg/L) exceeded the ice bottom value.

Compared to Ramfjorden, VMF and Billefjorden sea ice Chl *a* concentrations were significantly higher ($p < 0.05$ for each comparison) in the bottom 0-3 cm sections by one to two orders of magnitude. The two high Arctic fjords showed similar patterns at VMF1, VMF2, BF1 and BF2 with highest concentrations of Chl *a* in the 0-3 section. BF3 was the only station with lower concentrations in the bottom section of the ice cores compared to the water column.

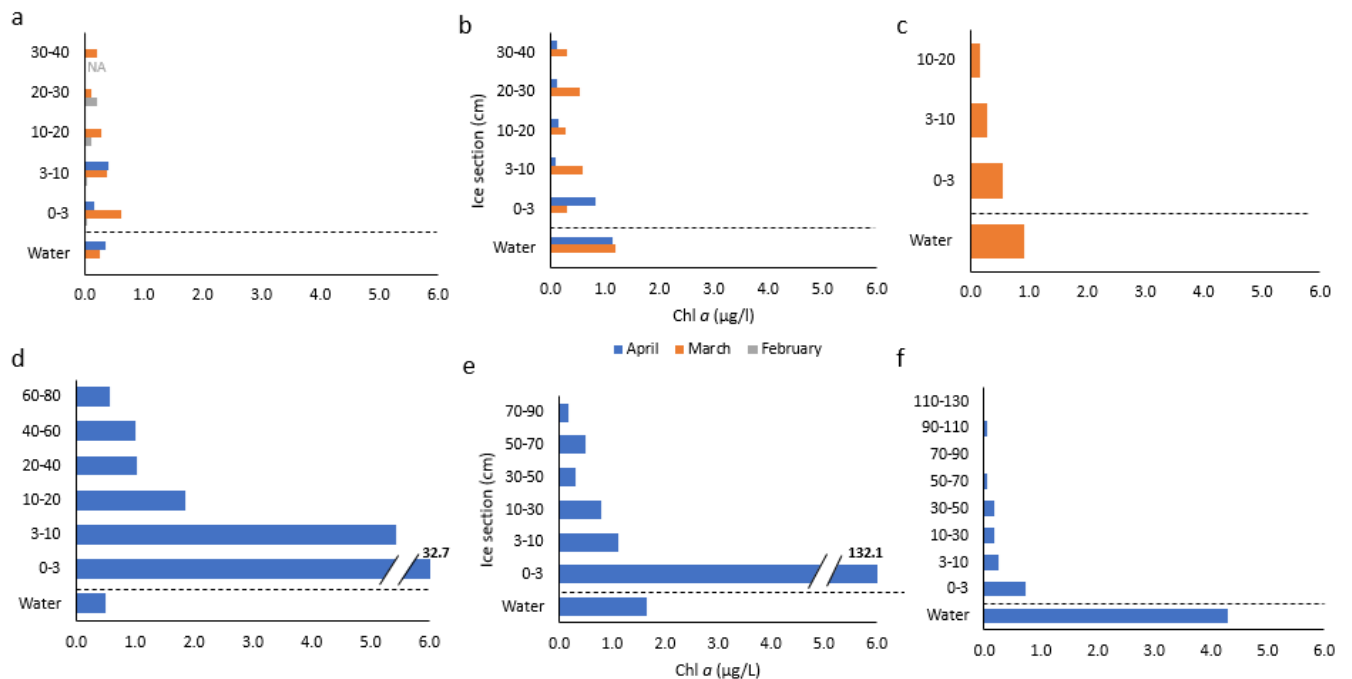


Figure 10. Chl *a* concentrations in the water column and in the ice core sections. a: RF1, b: RF3, c: RF5, d: VMF1, e: BF2, f: BF3. Data from additional stations can be found in Appendix F.

Bacterial abundance

In Ramfjorden, the abundance of bacteria was higher in the ice cores than in the water column at RF1-3 in February (Figure 11). Interestingly, February also showed the highest abundance of bacteria in the ice cores compared to all other months sampled with a range of 1.0×10^5 cells/ml to 3.2×10^6 cells/ml. The vertical distribution was highly variable within and between stations. The bacteria abundances decreased significantly ($p < 0.05$ each) from February to March at RF1-3 in the ice and water column. However, abundances at the additional March stations RF4 and RF5 were high in the ice cores (range: 3.6×10^5 - 3.0×10^6 cells/ml) (Appendix G). Abundances in April were similar to March data and ice abundances ranged from 1.0×10^4 to 6.0×10^4 cells/ml and the pelagic data ranged from 4.1×10^5 cells/ml to 6.5×10^5 cells/ml.

No adequate sampling occurred in Van Mijenfjorden and therefore bacteria abundance data are not available.

BF2 and BF3 had the highest abundance of bacteria in the water column while at BF1 the highest abundance was found in the ice bottom section (Figure 11). The water column data ranged from 2.4×10^5 cells/ml to 5.2×10^5 cells/ml while the ice cores had a wider range from 7.4×10^3 cells/ml to 1.4×10^6 cells/ml. Within the ice, the highest abundances of bacteria occurred in the bottom section at BF1 and BF2 while at BF3 the highest abundances were found in the ice interior. All stations in Billefjorden had the lowest abundances in the top sections of the ice cores.

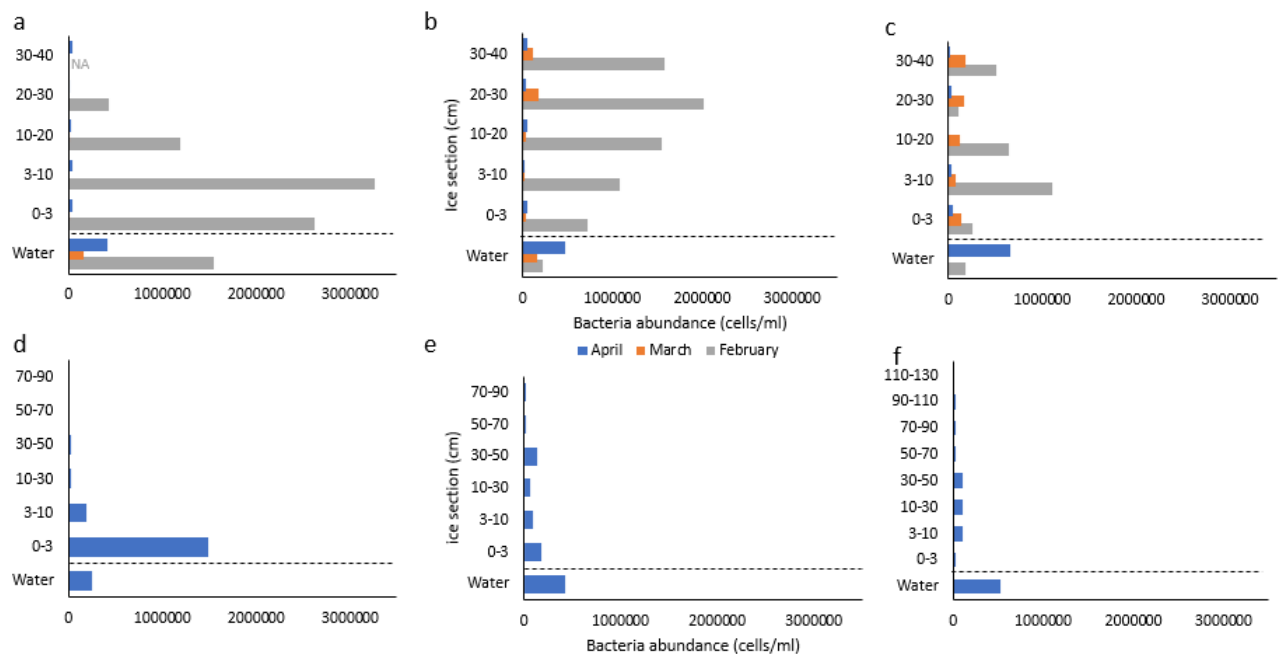


Figure 11. Bacteria abundance in the water column and in the ice core sections. a: RF1, b: RF2, c: RF3, d: BF1, e: BF2, f: BF3. Data from additional stations can be found in Appendix G.

All stations in Ramfjorden and Billefjorden, except BF1, had the highest abundance of bacteria in the water column in April with similar abundances ($p > 0.05$ each). BF1 was the only station that showed a clear vertical pattern with highest abundance in the bottom layer of the ice core while the other stations in April had a more homogenous vertical distribution of bacteria.

Algal abundance

Algal abundances in Ramfjorden showed a clear seasonal change with very low abundances in February and increases towards April (Figure 12). Both the ice cores (0.0 cells/L to 3.0×10^3 cells/L) and water samples (1.0×10^3 cells/L to 1.5×10^3 cells/L) had low or non-detectable algal abundances in February. However even in February, ice algae were detected in 78.6 % of all ice core sections. Algal abundances increased in all ice sections in March to values of 2.2×10^3 cells/L to 1.8×10^5 cells/L (Figure 12, Appendix H). Highest algal abundances were found in the top part of the cores except for RF4 where the highest abundance occurred in the bottom section of the ice. The phytoplankton abundance also increased during March (range: 1.6×10^3 - 1.5×10^5 cells/L) with the highest increase at RF3. The same vertical algal patterns could be seen in April as in March with highest algal abundances in the top parts of the ice cores. The ice cores in April had algal abundances ranging from 4.3×10^3 cells/L to 2.4×10^5 cells/L. Phytoplankton values increased once more in April at RF1, RF2 and RF3 with a range of 3.6×10^4 - 9.2×10^4 cells/L.

All stations in Van Mijenfjorden had the highest ice algal abundances in the bottom section of the ice cores and strongly decreasing abundances towards the top at VMF1 and VMF2 (Figure 12, Appendix H). The ice algal abundances ranged from 4.5×10^4 cells/L to 8.3×10^7 cells/L. The phytoplankton abundance were significantly lower (range: 1.6×10^4 - 1.1×10^5 cells/L) compared to the bottom section ($p < 0.05$ each) of the ice cores (range: 5.0×10^5 - 8.3×10^7 cells/L) at all Van Mijenfjorden stations.

The highest abundances of algae in Billefjorden was found in the bottom section at BF1 and BF2 (Figure 12, Appendix H). At these two stations, abundances followed a C-shaped pattern with the highest abundances at the bottom and top part of the ice core and lower abundances in the middle sections while BF3 had a more homogenous distribution of lower algal abundances throughout the core. Ice algal abundances throughout the ice cores ranged from 7.4×10^3 cells/L to 1.5×10^6 cells/L, exceeding ($p > 0.05$, each) the phytoplankton values at BF1 (2.6×10^5 cells/L) and BF2 (1.8×10^5 cells/L), specifically in the bottom section. At BF3,

phytoplankton abundances (8.8×10^5 cells/L) was above all ice algal abundances, similar to the patterns in Chl *a*.

All stations (except BF3) in Van Mijenfjorden and Billefjorden showed ice algal abundance maxima in the bottom part of the ice cores. Svalbard ice algal abundances were ca two magnitudes above the maximum values from Ramfjorden. In nearly all ice-covered stations, abundances of phytoplankton were lower compared to the highest algal abundances within the ice cores.

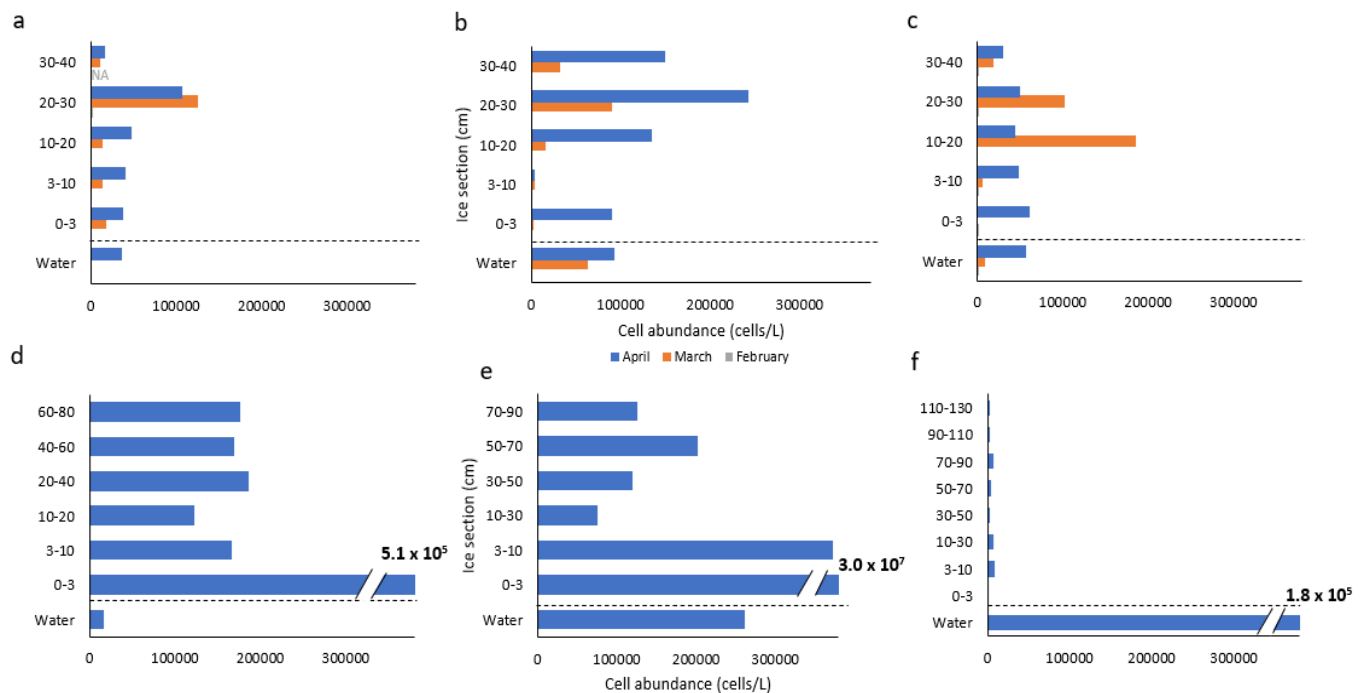


Figure 12. Cell abundance in the water column and in the ice core sections. a: RF1, b: RF2, c: RF3, d: VMF1, e: BF1, f: BF3. Data from additional stations can be found in Appendix H.

Community structure

A total of 11 taxa from 4 classes and 3 phyla were identified in sea ice and water samples from Ramfjorden (Table 2). 77.8% of the presented taxa were identified at the genus or species level, mainly Bacillariophyceae (within phylum Ochrophyta), while specifically for the very hard to identify flagellates, specimens were grouped into two size classes (5-15 μm and 15-40 μm). All Ramfjorden stations had similar taxonomic compositions in February with flagellates being the only taxon found in all ice sections and the water column (Figure 13, Appendix I) with the exception of the 20-30 cm section at RF3 with a 20% contribution of Bacillariophyceae dominated by *Leptocylindrus minimus*. A large increase in the relative contribution by Bacillariophyceae/Ochrophyta occurred at all stations in March where they contributed in the majority of ice sections at RF2 and RF3 over 50% of the total abundance.

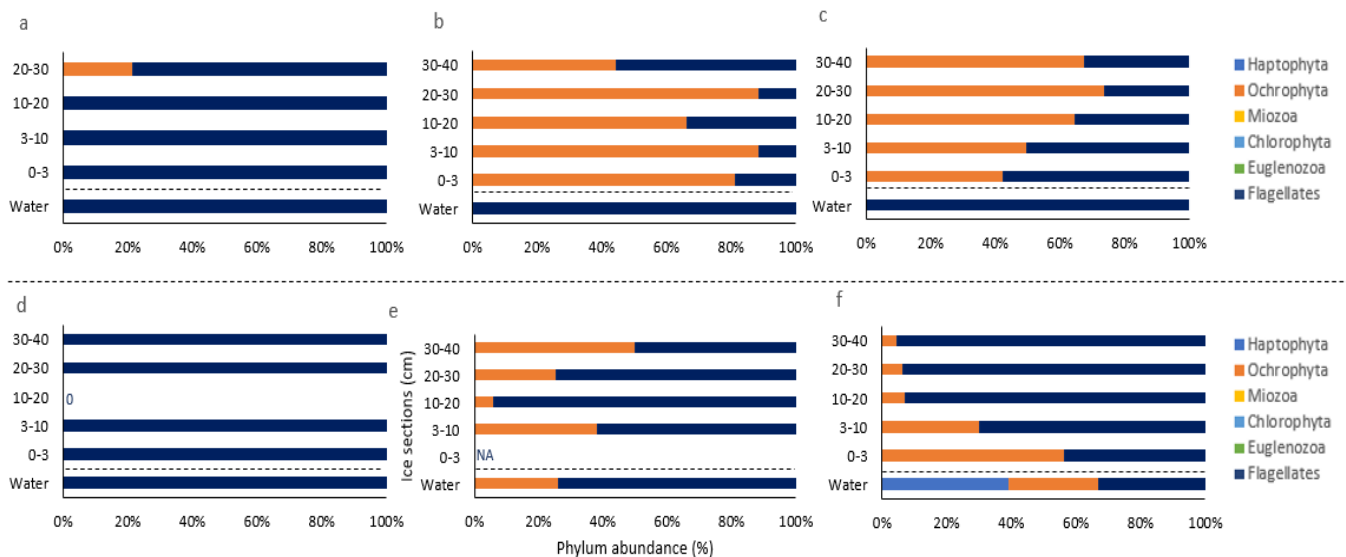


Figure 13. Relative contribution of different algal phyla in Ramfjorden from February to April. a: RF1, February, b: RF1, March, c: RF1, April, d: RF3, February, e: RF3, March, f: RF3, April. Data from additional stations can be found in Appendix I.

RF4 and RF5 in March had a similar community structure to RF1, RF2 and RF3 in February with a dominance of flagellates in the ice while the water column was dominated by Bacillariophyceae, mainly *Chaetoceros socialis*. In April, there was a shift back in dominance of flagellates at RF3 for all ice sections except the 0-3 cm section and the water column where *Nitzschia frigida* and *L. minimus* contributed ca 50% of total algal abundance. The dominating species in the phylum Ochrophyta in all ice sections was *L. minimus* with the exception of RF3 where *N. frigida* continued to dominate.

A total of 20 taxa from 6 classes and 5 phyla were identified in sea ice samples and water samples from Van Mijenfjorden. 85.0% of the taxa were identified to the genus or species level, mainly Bacillariophyceae, while unidentifiable flagellates were again grouped into two size classes (5-15 μm and 15-40 μm). The ice algal communities at Van Mijenfjorden were dominated by flagellates and Bacillariophyceae (Ochrophyta) at all three stations (Figure 14, Appendix I).

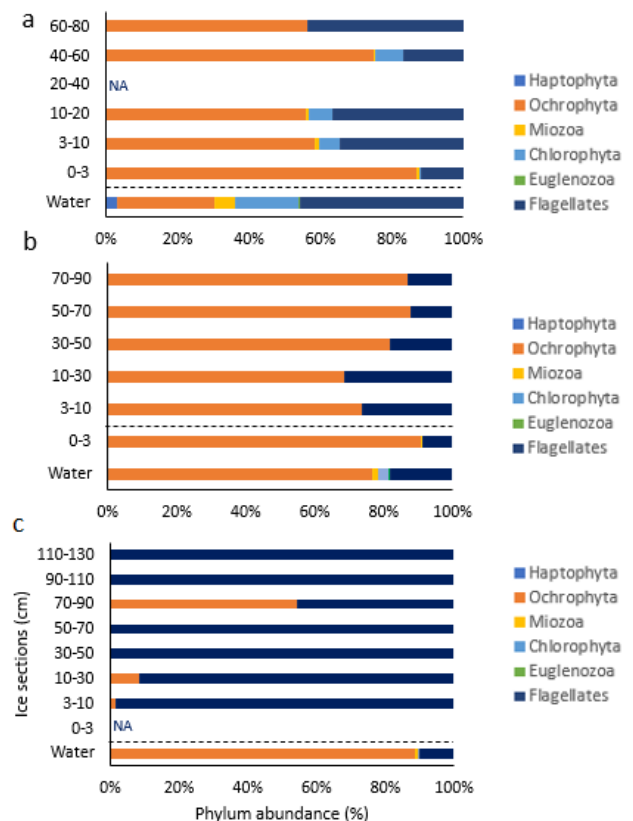


Figure 14. Relative contribution of different phyla to the algal composition in Van Mijenfjorden and Billefjorden. a: VMF1, April, b: BF1, April, c: BF3, April. Data from additional stations can be found in Appendix I.

Bacillariophyceae, mainly *Nitzschia frigida*, dominated in the bottom sections at all three stations exceeding >75% of the total abundance. Other species/genera in abundances > 2.0 x 10⁴ cells/l in the bottom sections were *Cylindrotheca closterium*, *Navicula vanhoefenii*, *Haslea* sp., *Entomoneis* sp. and unidentifiable small pennate diatoms with sizes up to 20 µm. Flagellates increased in abundance further up the core and a presence of Pyramimonadophyceae within the phylum Chlorophyta was seen at VMF1. The water column at RF2 was also dominated by Bacillariophyceae with relative contributions >50%, dominated mainly by *N. frigida* and smaller contributions of unidentified small pennate diatoms. The water column at VMF3 was dominated by flagellates while VMF1 had a more diverse distribution across taxa.

A total of 22 taxa from 5 classes and 4 phyla were identified in sea ice samples and water samples from Billefjorden (Table 2, Figure 14, Appendix I). 86.3% of the taxa were identified to the genus or species level, mainly Bacillariophyceae, with flagellates were grouped into two size classes (5-15 µm and 15-40 µm). BF1 and BF2 was dominated by Bacillariophyceae in all ice core sections with highest abundances by *N. frigida*, *C. closterium* and *N. vanhoefenii*. BF3 ice sections differed from the other two stations and were dominated by flagellates with the exception of the 70-90 cm section where Bacillariophyceae dominated with over 50%. Phytoplankton composition at all three stations was dominated by Bacillariophyceae, specifically *N. frigida*, *Fragilariopsis* sp., *Conscinodiscus* sp. and *C. socialis*.

Table 2. Species/taxa occurrence at the sampled stations.

Species	RF, Water	RF, Ice	VMF, Water	VMF, Ice	BF, Water	BF, Ice
<i>Chaetoceros socialis</i>	X	-	-	-	X	-
<i>Coscinodiscus</i> sp.	-	-	-	-	X	-
<i>Cylindrotheca closterium</i>	X	X	X	X	X	X
<i>Entomoneis</i> sp.	-	-	-	X	X	X
<i>Fragilariopsis cylindrus</i>	X	X	-	-	-	-
<i>Fragilariopsis</i> sp.	X	X	-	X	X	-
<i>Haslea</i> sp.	-	-	X	X	X	X
<i>Leptocylindrus minimus</i>	-	X	-	X	-	X
<i>Navicula granii</i>	-	-	X	X	X	X
<i>Navicula</i> sp.	-	-	X	X	X	X
<i>Navicula vanhoefenii</i>	-	-	-	X	X	X
<i>Nitzschia frigida</i>	-	X	X	X	X	X
Pennate diatoms, <20 µm	X	X	X	X	X	X
<i>Pleurosigma</i> sp.	-	-	X	X	X	X
<i>Thalassiosira nordenskiöldii</i>	-	-	-	-	X	-
<i>Alexandrium</i> sp.	-	-	X	X	X	X
<i>Amphidinium</i> sp.	-	-	X	-	X	X
<i>Dinophysis</i> sp.	X	-	-	-	-	-
<i>Gymnodinium</i> sp.	-	-	X	X	X	-
<i>Euglena</i> sp.	-	-	X	-	X	-
<i>Chattonella</i> sp.	-	-	X	X	X	X
<i>Phaeocystis pouchetii</i>	X	X	X	-	-	-
<i>Pyramimonas</i> sp.	-	-	X	X	X	-
Flagellates, 5-15 µm	X	X	X	X	X	X
Flagellates, 15-40 µm	X	X	X	X	X	X

The community structure of the sea ice and water samples differed substantially between the three fjords as can also be seen in the clear separation of Ramfjorden ice stations from those in Svalbard (Figure 15). Ramfjorden had a relatively homogenous flagellate dominated community in February. Algal diversity increased at the three stations in March and April with larger contributions of Bacillariophyceae where the dominating species was *L. minimus*. Van Mijenfjorden (8 genera) and Billefjorden (11 genera) had a larger richness of genera of Bacillariophyceae than Ramfjorden (5 genera) except for BF3 which had low diversity and similar community structure to Ramfjorden, where the dominance of flagellates and *L. minimus* could be seen (Figure 15). Van Mijenfjorden, BF1 and BF2 were closer in their sea ice algae community structures with species such as *N. frigida* and *Entomoneis* sp. being characteristic (Figure 15). The phytoplankton community in Ramfjorden was similar to the sea ice community in February and in Van Mijenfjorden but a succession in Ramfjorden with *Phaeocystis pouchetii*, *C. socialis* and dinoflagellates being characteristic could be seen in March and April. Billefjorden had two distinctly different communities in the water column and sea ice (Figure 15). The phytoplankton community in Billefjorden had a relatively high number of taxa and seven out of the 22 BF taxa were only found in the water column, e.g. *Coscinodiscus* sp., *Euglena* sp. and *Gymnodinium* sp. (Table 2).

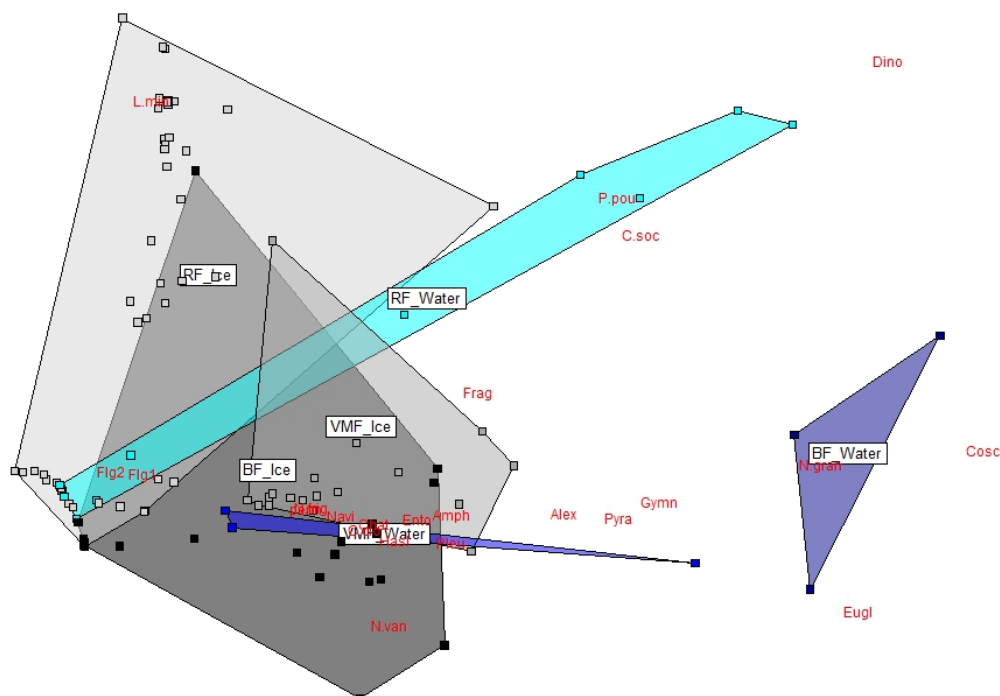


Figure 15. NMDS ordination of all ice/water samples based on the algal community structure. Stress value: 0.16. The abbreviated species names (in red) are build based on the first letter of the genus and the three first letters of the species (see Table 2 for full name) or the four first letters of the genus if identified only to genus level. The light blue area indicates RF water samples, while the two dark blue areas are BF/VMF water samples. All RF ice samples (light grey squares) are within the light grey area with BF ice samples in the dark grey (area and squares) and the VMF ice samples in medium grey (square and area).

Discussion

General outline of the discussion

The discussion will start with a focus on the physical and chemical variables within the sea ice environment. The following section on biological sea ice variables evaluates how the physical and chemical environmental properties in ice and sea water at the three sampled fjords shaped the associated algal communities. The methods used will thereafter be critically evaluated with suggestions for methodological improvements in future studies. At the end (conclusion), the major scientific outcome of this study is highlighted, initial hypotheses revisited and suggestions for future studies are proposed.

Physical and chemical variables

Snow plays a key role in structuring sea ice ecosystem through altering the physical environment compared to snow-free sea ice. Snow is a good insulator and therefore affects the heat budget of the ice (Petrich and Eicken 2016) and associated temperature distributions. A thick snow cover decreases the growth rate of the sea ice and alters the melting phase at the end of the season (Sturm and Massom 2016). It will also affect the temperatures within the ice with a thicker snow cover leading to smaller vertical temperature gradient (Arrigo 2014). Snow has an exceptionally high albedo (specifically for dry and cold snow) and also attenuation coefficient which directly affects the photosynthetic organisms in the sea ice as their phenology is largely controlled by light availability (Leu et al. 2015). In Ramfjorden, the snow depth increased every month sampled at all stations exceeding the mean snow depth at the Arctic areas in this study. This can be explained by the more humid climate in Ramfjorden which results in higher precipitation, 120.7 mm in April, 2019 (yr.no 2020 May 19), compared to the very dry high Arctic climate at Svalbard with only 30.3 mm in April, 2019 (yr.no 2020 May 19). The thicker snow in Ramfjorden also explains the generally weaker ice temperature related gradients (temperature, brine salinity) compared to the Arctic sites. Although not measured, a calculation of the light availability under the ice based on published attenuation coefficients and albedo values (Appendix J) indicates that light levels under the snow and ice in Ramfjorden in April were one to four order of magnitudes lower than those under the ice in Svalbard, leading to reduced growth potential of ice algae (Campbell *et al.*, 2018).

Sea ice growth and thickness changes are mainly dependent on the air/ocean heat exchange and consequently also linked to the air temperature, but also the depth of the snow cover

(Haas, 2017; Sturm and Massom, 2016). Although sea ice in Ramfjorden increased in thickness throughout the time series, it was significantly thinner than ice in Van Mijenfjorden and Billefjorden, which can be linked to the warmer ocean and air temperatures causing shorter and slower ice growth seasons compared to the high Arctic fast ice sites sampled in this study, and even more so compared to high Arctic multi-year ice, where thicknesses can be above 3 m in winter (Bourke and Garrett 1987). Ramfjorden was more similar to the sub-Arctic seasonally ice covered Baltic Sea which however typically has slightly thicker ice compared to Ramfjorden with a range ca. 0.35 to 0.70 m (Haecky and Andersson 1999). Thicker ice in the Baltic can be explained by the lower salinity of its surface water, which allows for faster growth rates compared to the more saline Norwegian fjords (e.g. Skardhamar and Svendsen 2010) and lower temperatures in the air, ranging from 0°C to -20°C (Haecky and Andersson 1999).

The temperature in the sea ice has two important effects on the sea ice biota. Cold sea ice temperatures require cold temperature adaptations of the polar ice biota in general (Thomas and Dieckmann 2002). Furthermore, ice temperature determines the brine salinity (Petrich and Eicken 2016) with increasing brine salinities (and smaller brine volume fractions) with decreasing temperatures (Niedrauer and Martin 1979; Leppäranta and Manninen 1988).

The decrease in the temperature gradient in Ramfjorden from February to March and April can be explained by the increased insulating snow depth in March to April (Arrigo 2014). The significantly lower ice temperatures at Van Mijenfjorden and Billefjorden were related to a thinner insulating snow cover and colder air temperatures in the Svalbard fjords (Sturm and Massom 2016). The warm temperature in the sea ice in March and April might have acted as a stressor for algae and bacteria that had adapted to the colder temperatures during the start of the ice-covered season.

Brine salinities are directly calculated from the ice temperatures, therefore brine salinities in the relatively warm sea ice in Ramfjorden were lower compared to the marine influenced Arctic areas like our Svalbard sites. However, they were close to observations from the northern Baltic Sea, where Haecky and Andersson (1999) determined brine salinities ranging from 2 to 12. The brine salinity is one of the most important factors that control the composition and distribution of organisms living in the ice as they have to adapt and acclimate to higher/lower salinities than in the water column (Gradinger and Bluhm 2018). The overall lower brine salinity and less strong gradients in Ramfjorden is likely a major

factor explaining the different species distribution and composition compared to Van Mijenfjorden and Billefjorden. A study by Zhang et al. (1999) showed that phytoflagellates had their highest growth at a salinity of 4 while pennate diatoms grew better in higher salinities. The Ramfjorden study did not differentiate between different flagellate taxa, however, based on Zhang et al. (1999), the low brine salinities would have led to higher growth rates for flagellates than diatoms, partially explaining the dominance of flagellates in Ramfjorden.

While bulk salinity is not representing directly the living conditions of ice biota, it is important through determining the brine volume (combined with ice temperature) and inhabitable ice space for ice biota (Cox and Weeks 1982; Granskog et al. 2006). It also determines the connectivity within the sea ice and with the ocean/air while these surrounding environments will affect the bulk salinity by e.g. ocean salinity, snow cover and ice surface flooding (Petrich and Eicken 2016). Newly formed sea ice has high bulk salinities of over 10, which decrease with the age of the ice due to brine drainage (Gradinger and Ikävalko 1998). Ramfjorden bulk salinities were well below those of first year ice in marine influenced Arctic areas where bulk salinities commonly are typically in a range of 5-8 (Arrigo, 2014; Svalbard stations in this study) but comparable to other freshwater influenced areas such as the Baltic Sea and Saroma Lagoon. Within Ramfjorden the river Sørbotnelva is located at the innermost part of the fjord and its run-off likely led to the increasing bulk salinities from station RF1 close to the river inlet to the more marine stations (e.g. RF3). Snow melting events or rain events could also have been a contributing factor in lowering the bulk salinity (Petrich and Eicken 2016). Overall, Ramfjorden bulk salinities were comparable to the northern Baltic Sea where bulk salinities are generally lower than 2 (Granskog et al. 2006) and also to Saroma Lagoon where a similar bulk salinity gradient from a river mouth and outwards was found with bulk salinities increasing from 1.7 to 8 (Robineau et al. 1997). This freshwater impact also explains the significantly lower bulk salinity at BF3, Billefjorden which was close to the freshwater discharge from a glacial front. Gravity driven desalination led to the decrease in the bulk salinity with season at all Ramfjorden stations. A thin layer of freshwater spreading under Ramfjorden sea ice (data not shown) could also reduce the bulk salinity already while the ice was forming.

The “law of fives” (Golden et al. 1998) stipulates that an ice temperature of -5°C , a bulk salinity of 5 and a resulting brine volume of 5% is the threshold between permeable and impermeable sea ice, controlling brine but also organism movement within the ice. More

applicable to freshwater influenced areas like Ramfjorden or the Baltic Sea (Thomas et al. 2017) is the “the law of ones” looking at temperatures of -1°C and bulk salinity of 1, developed by Leppäranta and Manninen (1988). The brine volume in Ramfjorden generally increased towards the marine stations where most ice was permeable during the whole time series, while the innermost stations generally were impermeable. The low brine volume fractions at the innermost stations were similar to those found in the Baltic Sea ice that on average range from 1.5% to 3.5% (Majaneva et al. 2017). This will have an effect on the organisms living in the sea ice both for their own movement but also limits new additions of fresh nutrients from the water column/snow when brine channels are not interconnected. In Ramfjorden, at BF3, but also in Baltic sea ice, low bulk salinities caused an overall low brine volume fraction (Granskog et al. 2006). The two high Arctic fast ice-covered fjords had significantly higher brine volumes and therefore overall higher permeability and more accessible space for biota. These differences in brine volume therefore confirms the initial hypothesis that ice algal biomass would be lower in Ramfjorden compared to the high Arctic fjords due to reduced inhabitable space. The lack of permeability would also prevent fresh supplies of nutrient e.g. from the water below into the ice which would affect the biomass accumulation. Interestingly, the glacial discharge impacted Billefjorden station BF3 was more similar to the Ramfjorden stations than the other high Arctic stations when comparing the brine volume likely due to the influence of freshwater discharge from the glacial front, combined with the warmer temperatures.

Nutrient availability is another critical variable that controls the growth of ice algae (Arrigo 2016). A shortage of nutrients will negatively affect the ice algal physiology and metabolism (Meiners and Michel 2016). This can occur specifically at later stages of the seasonal succession during high algal productivity in spring or during periods of limited input from external sources such as the seawater or snow deposit or in nutrient-depleted system conditions (Gradinger 2009).

The seasonal decrease of silicate concentrations in Ramfjorden can be caused by the observed growth of diatoms that use silicate to build up their frustules (Kooistra et al. 2007). An increasing gradient could be seen from the innermost station to the outer stations in all months. The two newly formed ice stations in March RF4 and RF5 had the highest concentrations, which is logical since algae had just been incorporated and no ice internal growth of diatoms had occurred. Additionally, the relatively young ice at these two stations had relatively high bulk salinities, which also explains higher silicate concentrations. The

silicate concentrations in April at Ramfjorden were similar to data from the Svalbard fjords. Interestingly, BF3 in Billefjorden had the overall highest silicate (and nitrate) concentration in both the sea ice and the water column compared to the other stations at the Svalbard fjords, which can be a result of nutrient additions through the subglacial outflow (Cape et al. 2019). The general temporal increase in nitrate in Ramfjorden could be caused by water advection into the fjord and/or an increased input from the snow cover that started to melt and added new nutrients to the sea ice. Nitrogen and phosphate are commonly deposited from the atmosphere onto the sea ice in the Baltic Sea and supplied to microalgae (Granskog et al. 2006). This process is likely not of high relevance to all parts within the ice in Ramfjorden, as its sea ice was generally not permeable throughout the whole ice core and new additions of nitrate from the snow would therefore stay in the top part of the core which can be seen at the outer stations. A phosphate reduction by algal growth (Townsend 2012) could be explained by the increased and relatively high Chl *a* concentrations in March when phosphate concentrations were the lowest. The N:P ratio in Ramfjorden during March and April indicates that phosphate was at limiting concentrations for algal growth (Redfield 1934) with ratios above 100 in a large number of ice core sections. Similar limitations have been reported for the Baltic Sea ice (e.g. Haecky et al. 1999; Piiparinen et al. 2010). The innermost station, RF3, had low concentrations of both phosphate and silicate in April which could have limited algal growth during this month leading to the decrease in diatom abundances.

Biological variables

Chlorophyll *a* is central for algal photosynthesis and is therefore one of the important variables to estimate algal growth (Townsend 2012) and biomass (Arrigo 2016).

Photosynthesis is light dependent and therefore altered by physical variables discussed above such as snow cover, leading to a large seasonal change in Chl *a* concentrations in sea ice (Leu et al. 2015). The highest concentrations of Chl *a* in high Arctic sea ice are generally seen at the ice-water interface as it provides sufficient light, supply of new nutrients from the ocean water below and lower salinity stress than in upper ice sections as outlined above (Cota and Smith 1991). Chl *a* showed a clear seasonal change in Ramfjorden sea ice. Very low concentrations in the water column in February indicates low organism incorporation into the growing sea ice. Phototrophic algal growth in January/beginning of February was restricted due to the lack of sufficient sunlight. Although surface irradiance increased in March/April, the thick snow depth in Ramfjorden caused a strong light reduction and while a small increase in Chl *a* could be seen in these months a strong spring peak was missing. Leu et al. (2015)

also report for the high Canadian Arctic that a deep snow depth (>20 cm) resulted in a permanent limitation of light for ice algae and a slow increase of Chl *a* concentrations without any visible peak compared to sites with less snow. The observed decrease of Chl *a* in April could be caused by brine flushing out of the warming ice or potentially consumption by sea ice herbivores (Bluhm et al. 2016) being able to access the wider brine channels. As typically grazing activity by sea ice meiofauna has little impact on sea ice algal biomass accumulation, it can be assumed that physical processes played the key role as observed also in Arctic pack ice studies (Gradinger et al. 1992). The absolute Chl *a* concentrations in Ramfjorden were at the detection limit or low during the whole time series compared to this studies Arctic fjord data and typical high Arctic fast ice systems (e.g. Gradinger et al. 2009) where concentrations in the bottom section of the ice can be two to three orders of magnitude higher than the maximum concentrations found in Ramfjorden. Although small, Ramfjorden Chl *a* biomass and the freshwater influenced station BF3 in Billefjorden were comparable to data from the northern Baltic Sea, where sea ice concentrations in the Gulf of Bothnia, northern Baltic Sea, were on average 3.0 µg/l or lower (Piiparinen et al. 2010). This suggests that the low Chl *a* concentrations in Ramfjorden during the spring months is caused mainly by two processes. First, the thick snow cover was a major limiting factor as less light reached the algae and therefore strongly reduced the rate of photosynthesis. Secondly the above outlined physical environmental stressors (also at BF3 in Billefjorden) constrained algal growth.

Marine heterotrophic bacteria depend on organic carbon primarily produced by algae and their activities are therefore tightly coupled (Seuthe et al. 2018). Bacteria are most likely, although not confirmed at this time, dependent on algal cells as carriers for incorporation into the sea ice. They can be physically enriched into the newly formed sea ice (Gradinger and Ikävalko 1998) and can occur in high abundances in many field studies (Deming and Eric Collins 2016). Bacteria, in contrast to algae, occurred in all ice sections sampled in Ramfjorden but in one to two orders of magnitude lower abundances compared to high Arctic sea ice sites in spring where abundances can exceed 10^7 cells/ml (Arrigo 2014). Winter Ramfjorden bacterial abundances in February and at the newly formed ice in March at RF4 and RF5 were similar to data from the northern Baltic Sea ice (Haecky and Andersson 1999) where a range of 7.0×10^4 - 2.7×10^5 cells/ml was detected from January to April. Abundances in the water column at all months at Ramfjorden were also only slightly lower than Baltic Sea pelagic data found in the same study where abundances ranged from 7.5×10^5 - 1.3×10^6 cells/ml. Interestingly, the abundances in March and April decreased within the ice and were

similar to low abundances from the upper parts of Arctic winter sea ice where low abundances of 4×10^3 cells/ml have been reported (Deming and Eric Collins 2016). Possible causes could be the low algal biomass and production within the Ramfjorden sea ice combined with environmental stress including low brine volume fraction and low brine salinities as well as low substrate availability. Here a future study could focus on the actual bacterial production rates and succession to elucidate the functional responses within the bacterial communities.

Sea ice algal cells are already incorporated into the growing ice sheet during ice formation (Gradinger and Ikävalko 1998) and further increase in abundance later in the season due to local growth. Similar to Chl *a*, the highest abundances of high Arctic sea ice algal species are often seen at the ice-water interface while lower abundances occur in the upper ice column where living conditions are more challenging (Arrigo 2016). Analysis of the community composition allows for insight to which species are better adapted to the ice specific local growth conditions in terms of e.g. high salinities, low temperatures and limited light (Gradinger and Bluhm 2018).

With the onset of light, an increase in algal abundances occurred also in Ramfjorden sea ice however with lower abundances compared to marine influenced Arctic fjords. Abundances in Svalbard fjords (this study) and in Arctic pack ice systems (e.g. Szymanski and Gradinger 2016) had more than two orders of magnitude higher abundances than the maximum abundances found in Ramfjorden – similar to the differences observed for Chl *a*. Algal incorporation in February was very low due to the low phytoplankton abundance. With season, both Chl *a* and abundances did increase. One major limiting factor in Ramfjorden compared to the high Arctic fjords was the thick snow cover which substantially delayed ice algal bloom formation (Leu et al. 2015). Indeed, most estimated light intensities using a basic light model indicated that less than 0.03% of the surface irradiance reached the algae at the bottom of the ice in April compared to the Svalbard fjords where all estimated relative light intensities were above 0.1% (Appendix J). Secondly, low salinities and brine flushing combined with potential grazing could limit algal growth as already discussed above (Ewert and Deming 2013; Bluhm et al. 2016). Highest abundance in the top part of the cores could be due to surface flooding of the ice as a result of the heavy snow cover, adding new cells to the top sections of the ice (Sturm and Massom 2016) similar to infiltration communities reported from the Arctic (Fernández-Méndez et al. 2018). Potentially, the higher light intensities in the upper parts of the ice cores in Ramfjorden could have allowed for higher in-situ growth in these layers.

The ice algal community structure in Ramfjorden changed over time from an almost complete dominance of flagellates to an overall dominance by diatoms. Diatoms are also the most abundant primary producers in both Baltic Sea ice (Thomas et al. 2017) and high Arctic sea ice systems (Gradinger and Bluhm 2018), able to tolerate a wide range of environmental gradients (Kooistra et al. 2007). A dominance of flagellates similar to Ramfjorden was also reported from the Baltic Sea (Piiparinen et al. 2010). Piiparinen et al. (2010) suggested that the dominance of small flagellates in the sea ice was due to the lack of habitable space for larger algal species. This hypothesis is supported by the Ramfjorden data where brine volumes were overall low and therefore likely not as suitable for larger algal groups such as diatoms. Here, an analysis of brine channel dimensions would allow to further address this question. Flagellate abundances and diversity can easily be underestimated, as the smaller flagellates are often difficult to identify using light-microscopy because of their small size and lack of distinct features as well as fixation artefacts. Here, molecular analyses can provide improved diversity estimates for all ice inhabitants and specifically flagellates, which are harder to identify compared to e.g. diatoms (Thomas et al. 2017). The succession within the ice from a dominance of flagellates to diatoms in Ramfjorden was clearly driven by ice internal factors (e.g. the age of the ice and in-ice algal growth) and not through interactions with a changing phytoplankton community in the water column. This can be seen in the March samples from the newly formed ice at RF4 and RF5, where the ice was still dominated by flagellates while the older ice at RF1 to RF3 had higher abundance of diatoms. This is surprising as the diatoms had been present within the phytoplankton community at RF4 and RF5. The typical high Arctic sea ice algal species *Nitzschia frigida* (e.g. Hop et al. 2020) dominated both in the water column and the bottom ice in Van Mijenfjorden and Billefjorden but also in northern Baltic Sea ice (Norrman and Andersson 1994). While it also occurred in high abundances in Ramfjorden at RF3 in March and April, the overall dominating diatom species had been *Leptocylindrus minimus*, leading to a clear separation of Ramfjorden ice communities from all others, also seen in the NMDS ordination. While this colony forming centric species has been observed both in the Arctic and in the Baltic Sea (Walter and Boxshall 2018) only few high Arctic reports provide evidence for a dominance of *L. minimus* in sea ice, for example in the Arctic Gyre by Melnikov (2005). *N. frigida* was actually absent at the most freshwater influenced station RF1, while *L. minimus* showed the opposite spatial trend with highest abundances at RF1 and at the intermediate station RF2. This could point towards different salinity tolerance of these two diatom species. The difference in salinity tolerance could also be supported by the NMDS ordination (Figure 15), where *L. minimus*

was characteristic for the low salinity water, Ramfjorden and BF3, while *N. frigida* was characteristic for Van Mijenfjorden, BF1 and BF2. Dominance of centric diatoms over pennate diatoms has also been reported in other sub-Arctic freshwater influenced areas such as the northern Baltic Sea (Piiparinen et al. 2010) and Saroma Lagoon (Robineau et al. 1997). Kikuchi-Kawanobe and Kudoh (1992) suggest that pennate diatoms might be generally better adapted to the high Arctic environmental settings and therefore dominate the sea ice in these areas while centric diatoms are better adapted to dominating in low latitude areas. For example, pennate diatoms are better adapted to darkness than centric diatoms (Piiparinen et al. 2010). Also, centric diatoms might benefit from an earlier light availability at low latitudes. Sensitivity to light can also be seen in Ramfjorden where under thick snow cover the highest abundances of *L. minimus* occurred in the top sections of the ice with higher light availability while *N. frigida* had higher abundances in the darker bottom sections of the ice.

The freshwater influenced Billefjord station BF3 showed a similar flagellate dominated community composition in the sea ice as Ramfjorden (as also supported by the NMDS ordination), but differed from the two other stations in Billefjorden. The similarity between Ramfjorden and BF3 are most likely a result of the large influence of freshwater compared to the two other stations in Billefjorden. In addition to freshwater as driving factor, BF3 could be in an earlier stage of the spring bloom community compared to the outer station, BF1, in Billefjorden that showed indication of being at the end of the spring bloom community with low primary production while biomass and the vertical flux of Chl *a* was high (T. Vonnahme personal communication, 2020 May 25).

Critique of methods

Standard techniques were used during the sampling and are in line with most other studies in the same field (Eicken 2009). The ice core samples taken during the warmer periods, especially in April, were very porous at the bottom and parts of the ice and specifically brine volume might therefore have been lost in the drilling process, underestimating organism abundances as well as changing all property measurements like salinity, nutrients, and Chl *a*. Increased sampling frequency, potentially to every second week, would allow to follow more clearly the processes in nutrient dynamics, sea ice changes, and biological properties. Future studies should include measurements of surface and under-ice irradiance, given the identified significance of this variable on algal growth.

The failure of the UiT CHN analyser caused the lack of data for this variable, although samples had been collected. This would have added valuable information on the seasonal increase in biomass and potential limitations as detectable through the C/N ratio.

The lack of personal experience concerning algae identification should also be taken into consideration, and the community structure from samples analysed at the beginning of the project might differ from the ones analysed at the end in their taxon resolution. Certainly, my confidence and knowledge in species identification increased over time and could lead to increased number of lower taxonomic levels. Also, application of molecular tools could have been useful. Most Lugol fixed samples from Van Mijenfjorden and Billefjorden were accidentally put into a freezer on RV *Helmer Hansen*, when being transported back to Tromsø. This might have affected cell structures, however I do not expect a difference in the identification of taxa with hard frustules (diatoms), but flagellates might have been underestimated for the Arctic fast ice samples.

Conclusions

The main aim of this thesis was to investigate the sea ice environment and biology in Ramfjorden and compare this information to data from other Arctic and sub-Arctic areas. Overall, the study showed the presence of an active community of bacteria and eukaryotic algae within the Ramfjorden ice, with strong seasonal and spatial gradients related to the environmental settings. Interestingly, the similar physical/chemical/biological properties in freshwater influenced ice systems including Ramfjorden, Billefjorden station BF3 and for example the northern Baltic Sea were distinctly different from typical marine high Arctic sea ice systems. Here, low bulk salinities and brine volume fractions, combined with warm temperatures and low brine salinities were important environmental stressors. The very high snow load in Ramfjorden reduced light intensities to levels where algal growth was severely limited. Unique and distinctly different communities and/or abundance levels of bacteria and algae compared to pelagic samples developed with clear seasonal changes in Ramfjorden sea ice. The algal community showed a succession from a dominance of flagellates in the dark early ice season to an increasing abundance of mainly centric diatoms similar to e.g. the northern Baltic Sea. The dominant diatom species in almost all ice sections was *Leptocylindrus minimus*, but common Arctic species such as *Nitzschia frigida* were also found. Many biological sea ice related research questions could be addressed using Ramfjorden ice as a test bed. It would be interesting to have a closer look at the bacterial community in Ramfjorden in order to understand why, opposite to both the Arctic and the

northern Baltic Sea, abundances decreased with the season. It remains unknown whether any metazoans live in the Ramfjorden sea ice and feed on the present ice algae. A suggestion for future studies in Ramfjorden would be to focus on the taxonomy and activity of flagellates in the sea ice and identify their composition with the help of molecular analyses. Additional research questions could look at the role of the freshwater run-off influencing the sea ice systems. Here Ramfjorden might offer an opportunity for easy-to-access experimental studies, which might help to elucidate the future of similarly freshwater influenced high Arctic systems.

References

- Arrigo KR. 2014. Sea Ice Ecosystems. *Ann Rev Mar Sci.* 6:439–467. doi:10.1146/annurev-marine-010213-135103.
- Arrigo KR. 2016. Sea ice as a habitat for primary producers. In: Thomas DN, editor. *Sea Ice*. 3rd ed. Chichester, UK: John Wiley & Sons, Ltd. p. 352–369.
- Berge J, Renaud PE, Darnis G, Cottier F, Last K, Gabrielsen TM, Johnsen G, Seuthe L, Weslawski JM, Leu E, et al. 2015. In the dark: A review of ecosystem processes during the Arctic polar night. *Prog Oceanogr.* 139:258–271. doi:10.1016/j.pocean.2015.08.005.
- Bluhm BA, Swadling KM, Gradinger R. 2016. Sea ice as a habitat for macrograzers. In: Thomas DN, editor. *Sea Ice*. 3rd ed. Chichester, UK: John Wiley & Sons, Ltd. p. 394–414.
- Bourke RH, Garrett RP. 1987. Sea ice thickness distribution in the Arctic Ocean. *Cold Reg Sci Technol.* 13:259–280. doi:10.1016/0165-232X(87)90007-3.
- Campbell K, Mundy CJ, Belzile C, Delaforge A, Rysgaard S. 2018. Seasonal dynamics of algal and bacterial communities in Arctic sea ice under variable snow cover. *Polar Biol.* 41:41–58. doi:10.1007/s00300-017-2168-2.
- Cape MR, Straneo F, Beird N, Bundy RM, Charette MA. 2019. Nutrient release to oceans from buoyancy-driven upwelling at Greenland tidewater glaciers. *Nat Geosci.* 12:34–39. doi:10.1038/s41561-018-0268-4.
- Cota GF, Smith REH. 1991. Ecology of bottom ice algae: II. Dynamics, distributions and productivity. *J Mar Syst.* 2:279–295. doi:10.1016/0924-7963(91)90037-U.
- Cottier FR, Nilsen F, Skogseth R, Tverberg V, Skardhamar J, Svendsen H. 2010. Arctic fjords: A review of the oceanographic environment and dominant physical processes. *Geol Soc Spec Publ.* 344:35–50. doi:10.1144/SP344.4.
- Cox GFN, Weeks WF. 1982. Equations for determining the gas and brine volumes in sea ice samples. *J Glaciol.* 29:306–316. doi:10.1017/S0022143000008364.
- Deming JW, Collins ER. 2016. Sea ice as a habitat for Bacteria, Archaea and viruses. In: Thomas DN, editor. *Sea Ice*. 3rd ed. Chichester, UK: John Wiley & Sons, Ltd. p. 326–351.
- Eicken H. 2009. Ice sampling and basic sea ice core analysis. In: Eicken H, Gradinger R, Salganek M, Shirasawa K, Perovich D, Leppäranta M, editors. *Field Techniques for Sea Ice*

Research. Fairbanks: University of Alaska Press. p. 117–140.

Ewert M, Deming JW. 2013. Sea ice microorganisms: Environmental constraints and extracellular responses. *Biol.* 2:603–628. doi:10.3390/biology2020603.

Fer I, Widell K. 2007. Early spring turbulent mixing in an ice-covered Arctic fjord during transition to melting. *Cont Shelf Res.* 27:1980–1999. doi:10.1016/j.csr.2007.04.003. [

Fernández-Méndez M, Olsen LM, Kauko HM, Meyer A, Rösel A, Merkouriadi I, Mundy CJ, Ehn JK, Johansson AM, Wagner PM, et al. 2018. Algal hot spots in a changing Arctic Ocean: Sea-ice ridges and the snow-ice interface. *Front Mar Sci.* 5(MAR). doi:10.3389/fmars.2018.00075.

Garrison DL, Close AR, Reimnitz E. 1989. Algae concentrated by frazil ice: Evidence from laboratory experiments and field measurements. *Antarct Sci.* 1:313–316. doi:10.1017/S0954102089000477.

Golden KM, Ackley SF, Lytle VI. 1998. The percolation phase transition in sea ice. *Science* 5387:2238–2241. doi:10.1126/science.282.5397.2238.

Gradinger R. 2009. Sea-ice algae: Major contributors to primary production and algal biomass in the Chukchi and Beaufort Seas during May/June 2002. *Deep Res Part II Top Stud Oceanogr.* 56:1201–1212. doi:10.1016/j.dsr2.2008.10.016.

Gradinger R, Ikävalko J. 1998. Organism incorporation into newly forming arctic sea ice in the greenland sea. *J Plankton Res.* 20:871–886. doi:10.1093/plankt/20.5.871.

Gradinger R, Bluhm B. 2018. Sea ice, a unique habitat in Svalbard's seas. In: Wassmann P, editor. *At the edge...* 1st ed. Stamsund: Orkana forlag. p. 167–175.

Gradinger R, Spindler M, Weissenberger J. 1992. On the structure and development of Arctic pack ice communities in Fram Strait: a multivariate approach. *Polar Biol.* 12:727–733. doi:10.1007/BF00238874.

Gradinger RR, Kaufman MR, Bluhm BA. 2009. Pivotal role of sea ice sediments in the seasonal development of near-shore Arctic fast ice biota. *Mar Ecol Prog Ser.* 394:49–63. doi:10.3354/meps08320.

Granskog MA, Kaartokallio H. 2004. An estimation of the potential fluxes of nitrogen, phosphorus, cadmium and lead from sea ice and snow in the northern Baltic Sea. *Water Air*

Soil Pollut. 154:331–347. doi:10.1023/B:WATE.0000022975.74321.27.

Granskog M, Kaartokallio H, Kuosa H, Thomas DN, Vainio J. 2006. Sea ice in the Baltic Sea - A review. *Estuar Coast Shelf Sci.* 70:145–160. doi:10.1016/j.ecss.2006.06.001.

Grossmann S, Gleitz M. 1993. Microbial responses to experimental sea-ice formation: Implications for the establishment of Antarctic sea-ice communities. *J Exp Mar Bio Ecol.* 173:273–289. doi:10.1016/0022-0981(93)90058-V.

Grossmann S, Dieckmann GS. 1994. Bacterial standing stock, activity, and carbon production during formation and growth of sea ice in the Weddell Sea, Antarctica. *Appl Environ Microbiol.* 60:2746–2753.

Haas C. 2016. Sea ice thickness distribution. In: Thomas DN, editor. *Sea Ice*. 3rd ed. Chichester, UK: John Wiley & Sons, Ltd. p. 42–64.

Haecky P, Andersson A. 1999. Primary and bacterial production in sea ice in the northern Baltic Sea. *Aquat Microb Ecol.* 20:107–118. doi:10.3354/ame020107.

Haecky P, Jonson S, Andersson A. 1999. Influence of sea ice on the composition of the spring phytoplankton bloom in the northern Baltic Sea. *Polar Biol.* 21:128. doi:10.1007/s003000050343.

Hop H, Vihtakari M, Bluhm BA, Assmy P, Poulin M, Gradinger R, Peeken I, von Quillfeldt C, Olsen LM, Zhitina L, et al. 2020. Changes in Sea-Ice Protist Diversity With Declining Sea Ice in the Arctic Ocean From the 1980s to 2010s. *Front Mar Sci.* 7. doi:10.3389/fmars.2020.00243.

Howe JA, Austin WEN, Forwick M, Paetzel M, Harland R, Cage AG. 2010. Fjord systems and archives: A review. *Geol Soc Spec Publ.* 344:5–15. doi:10.1144/SP344.2.

Høyland K V. 2009. Ice thickness, growth and salinity in Van Mijenfjorden, Svalbard, Norway. *Polar Res.* 28:339–352. doi:10.1111/j.1751-8369.2009.00133.x.

Johnsen G, Leu E, Gradinger R. 2020. Marine Micro- and Macroalgae in the Polar Night. In: Berge J, Johnsen G, Cohen J, editors. *Polar Night Marine Ecology*. 1st ed. Cham: Springer International Publishing. p. 67–112.

Kaartokallio H, Granskog MA, Kuosa H, Vainio J. 2016. Ice in subarctic seas. In: Thomas DN, editor. *Sea Ice*. 3rd ed. Chichester, UK: John Wiley & Sons, Ltd. p. 630–644.

- Kartverket. 2015. Sjøkart - Dybdata - Kartkatalogen. [accessed 2020 May 27].
<https://kartkatalog.geonorge.no/metadata/kartverket/dybdata/2751aacf-5472-4850-a208-3532a51c529a>.
- Kartverket. 2018. Open and free geospatial data from Norway. [accessed 2020 May 19].
<https://www.kartverket.no/en/data/Open-and-Free-geospatial-data-from-Norway/>.
- Kikuchi-Kawanobe K, Kudoh S. 1992. Species composition of ice algal assemblages in Saroma Ko lagoon and resolute passage, 1992 (extended abstract). *Proc NIPR Symp Polar Biol.* 8:59–63.
- Kooistra WHCF, Gersonde R, Medlin LK, Mann DG. 2007. The Origin and Evolution of the Diatoms: Their Adaptation to a Planktonic Existence. In: Falkowski PG, Knoll AH, editors. *Evolution of Primary Producers in the Sea*. 1st ed. San Diego: Elsevier. p. 207–249.
- Krawczyk DW, Witkowski A, Juul-Pedersen T, Arendt KE, Mortensen J, Rysgaard S. 2015. Microplankton succession in a SW Greenland tidewater glacial fjord influenced by coastal inflows and run-off from the Greenland Ice Sheet. *Polar Biol.* 38:1515–1533.
doi:10.1007/s00300-015-1715-y.
- Krembs C, Gradinger R, Spindler M. 2000. Implications of brine channel geometry and surface area for the interaction of sympagic organisms in Arctic sea ice. *J Exp Mar Bio Ecol.* 243:55–80. doi:10.1016/S0022-0981(99)00111-2.
- Lange MA, Ackley SF, Wadhams P, Dieckmann GS, Eicken H. 1989. Development of sea ice in the Weddell Sea. *Ann Glaciol.* 12:92–96. doi:10.3189/s0260305500007023.
- Van Leeuwe MA, Tedesco L, Arrigo KR, Assmy P, Campbell K, Meiners KM, Rintala JM, Selz V, Thomas DN, Stefels J. 2018. Microalgal community structure and primary production in Arctic and Antarctic sea ice: A synthesis. *Elementa.* 6. doi:10.1525/elementa.267.
- Leppäranta M, Manninen T. 1988. The brine and gas content of sea ice with attention to low salinities and high temperatures. *Finnish Inst Mar Res Intern Rep.* 2:1–14.
- Leu E, Mundy CJ, Assmy P, Campbell K, Gabrielsen TM, Gosselin M, Juul-Pedersen T, Gradinger R. 2015. Arctic spring awakening - Steering principles behind the phenology of vernal ice algal blooms. *Prog Oceanogr.* 139:151–170. doi:10.1016/j.pocean.2015.07.012.
- Majaneva M, Blomster J, Müller S, Autio R, Majaneva S, Hyytiäinen K, Nagai S, Rintala JM. 2017. Sea-ice eukaryotes of the Gulf of Finland, Baltic Sea, and evidence for herbivory on

- weakly shade-adapted ice algae. *Eur J Protistol.* 57:1–15. doi:10.1016/j.ejop.2016.10.005.
- Meiners KM, Michel C. 2016. Dynamics of nutrients, dissolved organic matter and exopolymers in sea ice. In: Thomas DN, editor. *Sea Ice*. 3rd ed. Chichester, UK: John Wiley & Sons, Ltd. p. 415–432.
- Melnikov IA. 2005. Sea ice-upper ocean ecosystems and global changes in the Arctic. *Russ J Mar Biol.* 31:1–8. doi:10.1007/s11179-006-0010-8.
- Niedrauer TM, Martin S. 1979. An experimental study of brine drainage and convection in Young Sea ice. *J Geophys Res.* 84:1176. doi:10.1029/jc084ic03p01176.
- Nilsen F, Cottier F, Skogseth R, Mattsson S. 2008. Fjord-shelf exchanges controlled by ice and brine production: The interannual variation of Atlantic Water in Isfjorden, Svalbard. *Cont Shelf Res.* 28:1838–1853. doi:10.1016/j.csr.2008.04.015.
- Noji TT, Noji CIM, Barthel KG. 1993. Pelagic-benthic coupling during the onset of winter in a northern Norwegian fjord. Carbon flow and fate of suspended particulate matter. *Mar Ecol Prog Ser.* 93:89–99. doi:10.3354/meps093089.
- Norrman B, Andersson A. 1994. Development of ice biota in a temperate sea area (Gulf of Bothnia). *Polar Biol.* 14:531–537. doi:10.1007/BF00238222.
- NPI. 2017. Norwegian Polar Institute: Map Data and Services. [accessed 2020 May 27]. <https://geodata.npolar.no/>.
- Oksanen J, Roeland K, Legendre P, O’Hara B, Stevens MHH, Oksanen J, Suggest M. 2007. The vegan package. *Community Ecol Packag.* 10:631–637.
- Olsen LM, Laney SR, Duarte P, Kauko HM, Fernández-Méndez M, Mundy CJ, Rösel A, Meyer A, Itkin P, Cohen L, et al. 2017. The seeding of ice algal blooms in Arctic pack ice: The multiyear ice seed repository hypothesis. *J Geophys Res Biogeosciences.* 122:1529–1548. doi:10.1002/2016JG003668.
- Petrich C, Eicken H. 2016. Overview of sea ice growth and properties. In: Thomas DN, editor. *Sea Ice*. 3rd ed. Chichester, UK: John Wiley & Sons, Ltd. p. 1–41.
- Piiparinen J, Kuosa H, Rintala JM. 2010. Winter-time ecology in the Bothnian Bay, Baltic Sea: Nutrients and algae in fast ice. *Polar Biol.* 33:1445–1461. doi:10.1007/s00300-010-0771-6.

- Porter KG, Feig YS. 1980. The use of DAPI for identifying and counting aquatic microflora. *Limnol Oceanogr.* 25:943–948. doi:10.4319/lo.1980.25.5.0943.
- R Core Team. 2020. R: A language and environment for statistical computing. <https://www.r-project.org/>.
- Redfield AC. 1934. On the Proportions of Organic Derivatives in Sea Water and Their Relation to the Composition of Plankton. Univ Press Liverpool, James Johnstone Meml Vol.:1767–192. doi:citeulike-article-id:11236440.
- Robineau B, Legendre L, Kishino M, Kudoh S. 1997. Horizontal heterogeneity of microalgal biomass in the first-year sea ice of Saroma-ko Lagoon (Hokkaido, Japan). *J Mar Syst.* 11:81–91. doi:10.1016/S0924-7963(96)00030-9.
- Seuthe L, Bratbak G, Larsen A. 2018. Doing everything everywhere all the time - the story about those that were thought to be unimportant in the Arctic Ocean. In: Wassman P, editor. *At the edge...* 1st ed. Stamsund: Orkana forlag. p. 177–183.
- Skardhamar J, Svendsen H. 2010. Short-term hydrographic variability in a stratified Arctic fjord. *Geol Soc Spec Publ.* 344:51–60. doi:10.1144/SP344.5.
- Spindler M. 1994. Notes on the biology of sea ice in the Arctic and Antarctic. *Polar Biol.* 14:319–324. doi:10.1007/BF00238447.
- Staley JT, Gosink JJ. 1999. Poles Apart: Biodiversity and Biogeography of Sea Ice Bacteria. *Annu Rev Microbiol.* 53:189–215. doi:10.1146/annurev.micro.53.1.189.
- Sturm M, Massom RA. 2016. Snow in the sea ice system: friend or foe? In: Thomas DN, editor. *Sea Ice.* 3rd ed. Chichester, UK: John Wiley & Sons, Ltd. p. 65–109.
- Syvitski JPM, Burrell DC, Skei JM. 1987. *Fjords: Processes and products.* New York, NY: Springer New York.
- Szczuciński W, Zajaczkowski M, Scholten J. 2009. Sediment accumulation rates in subpolar fjords - Impact of post-Little Ice Age glaciers retreat, Billefjorden, Svalbard. *Estuar Coast Shelf Sci.* 85:345–356. doi:10.1016/j.ecss.2009.08.021.
- Szymanski A, Gradinger R. 2016. The diversity, abundance and fate of ice algae and phytoplankton in the Bering Sea. *Polar Biol.* 39:309–325. doi:10.1007/s00300-015-1783-z.
- Thomas DN, Dieckmann GS. 2002. Antarctic sea ice - A habitat for extremophiles. *Science*

295(5555):641–644. doi:10.1126/science.1063391.

Thomas DN, Kaartokallio H, Tedesco L, Majaneva M, Piiparinen J, Eronen-Rasimus E, Rintala J-M, Kuosa H, Blomster J, Vainio J, et al. 2017. Life associated with Baltic Sea ice. In: Snoeijs-Leijonmalm P, Schubert H, Radziejewska T, editors. *Biological oceanography of the Baltic Sea*. 1st ed. Dordrecht: Springer Netherlands. p. 333–357.

Thronsen J, Rytter Hasle G, Tangen K. 2007. *Phytoplankton of Norwegian Coastal Waters*. Oslo: Almatel Forlag AS.

Tomas CR. 1997. *Identifying Marine Phytoplankton*. San Diego: Elsevier.

Townsend DW. 2012. Introduction to Life in the Sea. In: *Oceanography and Marine Biology*. 1st ed. Sunderland: Sinauer Associates. p. 226–259.

Turner Designs. 2019. *Trilogy Laboratory Fluorometer User's Manual*. San Jose, CA. www.turnerdesigns.com.

Utermöhl H. 1958. Methods of collecting plankton for various purposes are discussed. *SIL Commun* 1953-1996. 9:1–38. doi:10.1080/05384680.1958.11904091.

Vihtakari M. 2020. PlotSvalbard: PlotSvalbard - Plot research data from Svalbard on maps. <https://github.com/MikkoVihtakari/PlotSvalbard>.

Walter TC, Boxshall G. 2018. *Worms : World Register of Marine Species*. [accessed 2020 May 3]. <http://www.marinespecies.org/aphia.php?p=taxdetails&id=149039#distributions>.

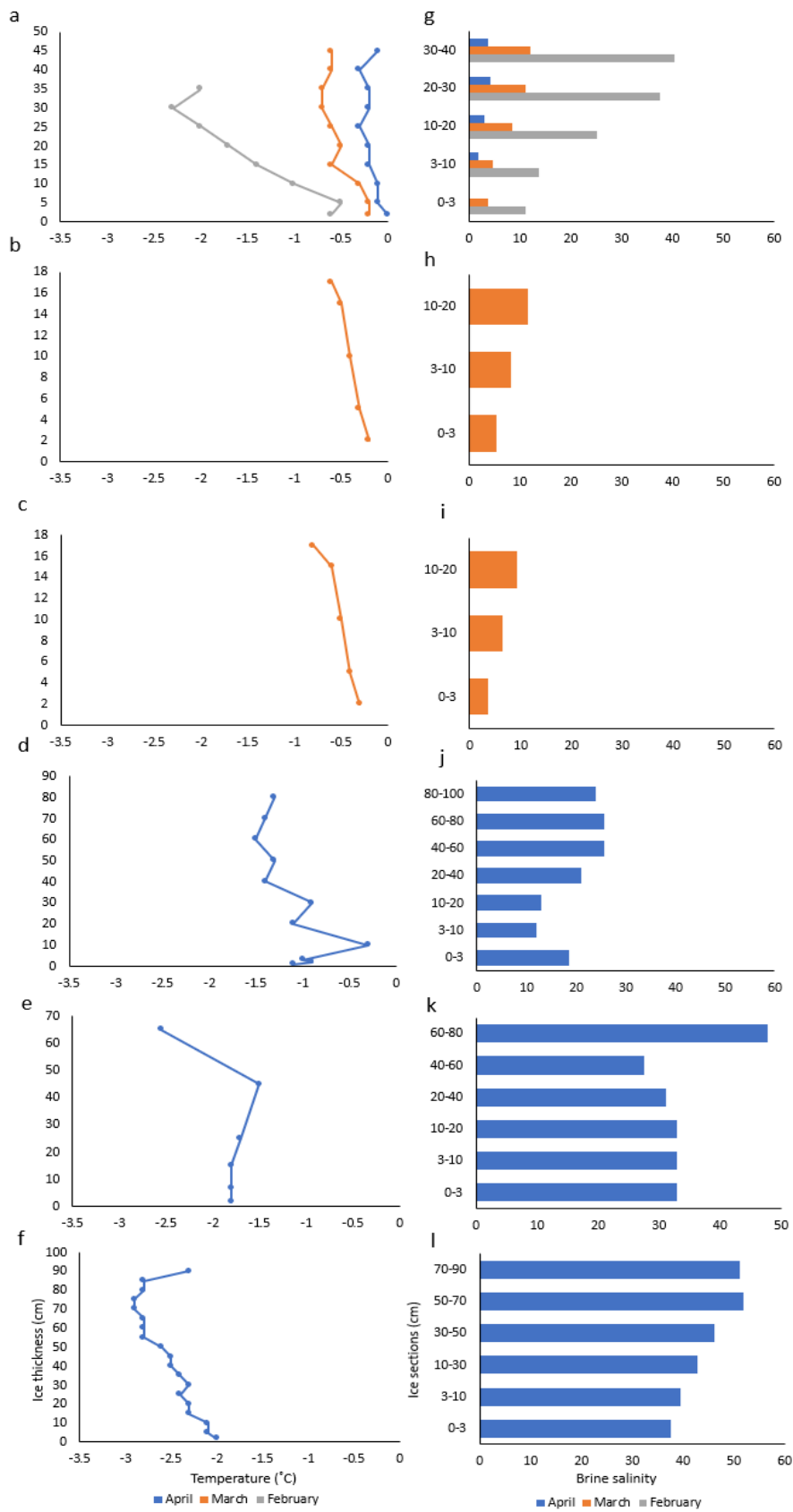
Weissenberger J, Dieckmann G, Gradinger R, Spindler M. 1992. Sea ice: A cast technique to examine and analyze brine pockets and channel structure. *Limnol Oceanogr*. 37:179–183. doi:10.4319/lo.1992.37.1.0179.

yr.no. Tromsø - historikk. [accessed 2020a May 19]. <https://www.yr.no/nb/historikk/graf/1-305409/Norge/Troms og Finnmark/Tromsø/Tromsø?q=2019-04>.

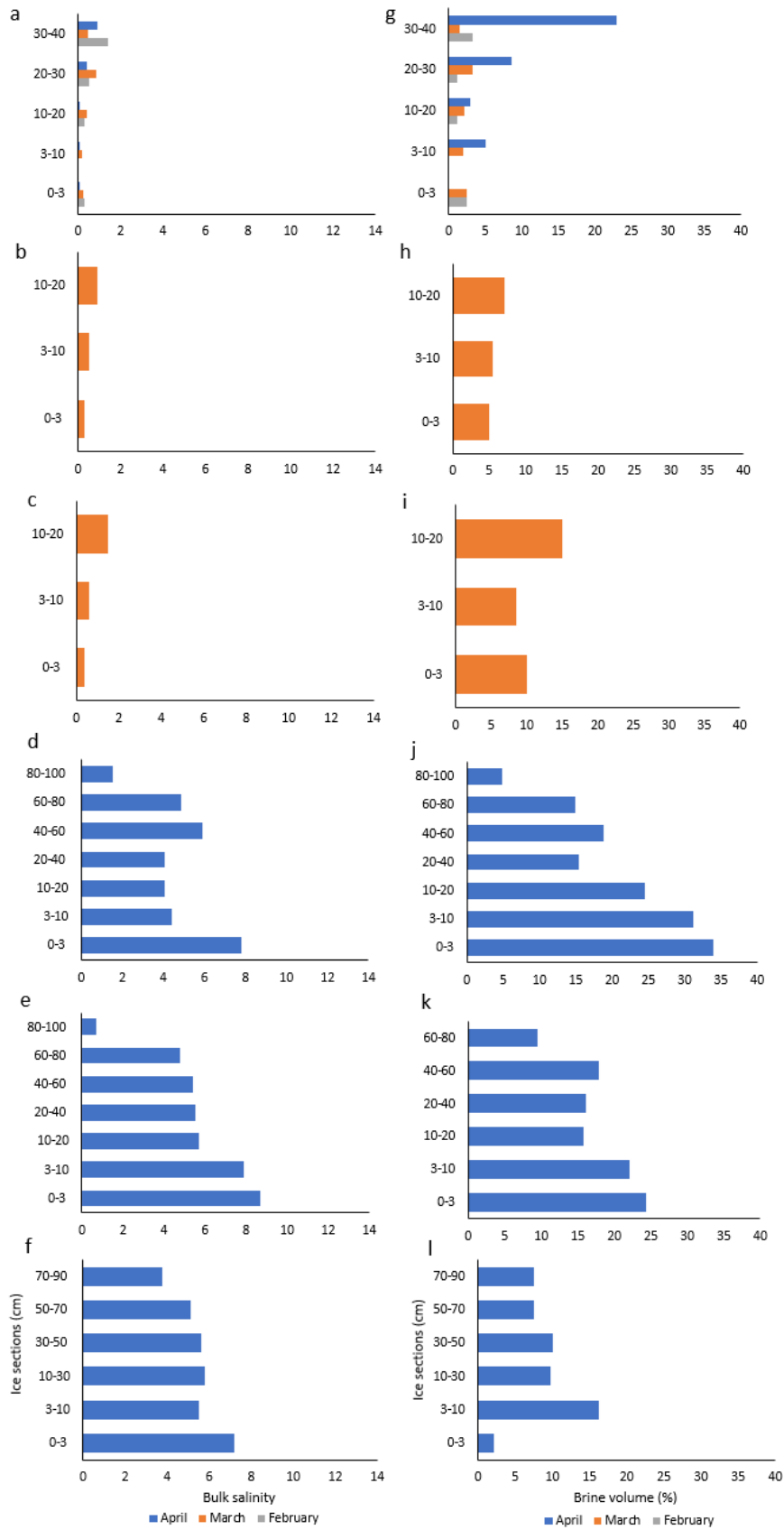
yr.no. Longyearbyen - historikk. [accessed 2020b May 19]. <https://www.yr.no/nb/historikk/graf/12759929/Norge/Svalbard/Svalbard/Longyearbyen?q=2020-03>.

Zhang Q, Gradinger R, Spindler M. 1999. Experimental study on the effect of salinity on growth rates of Arctic-sea-ice algae from the Greenland Sea. *Boreal Environ Res*. 4:1–8.

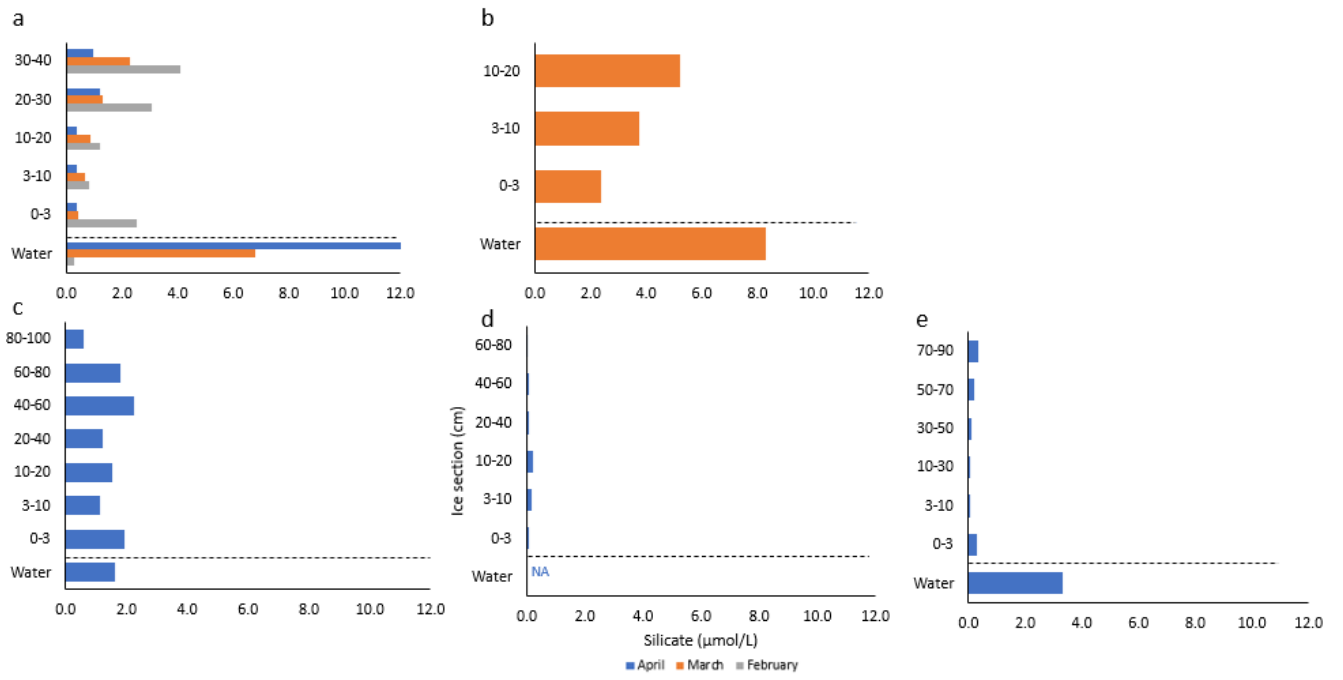
Appendix



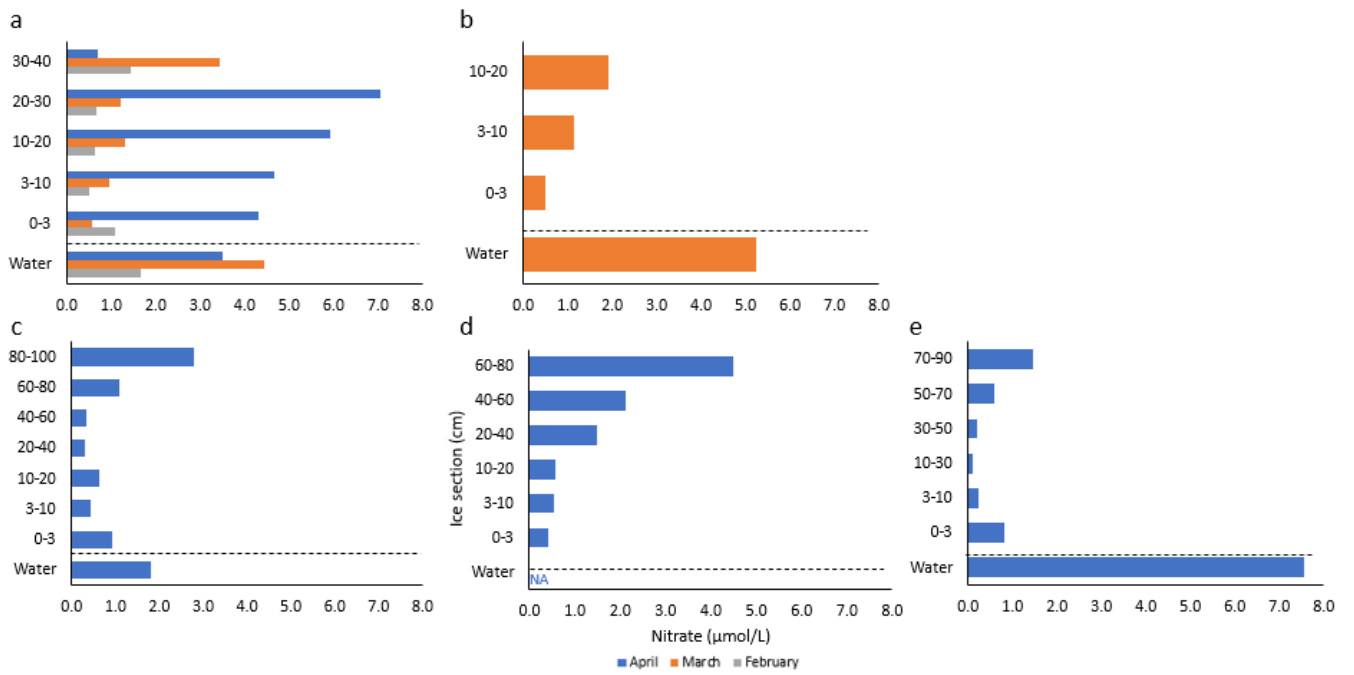
Appendix A. Vertical temperatures (left) and calculated brine salinity gradients in the ice cores (right). a&g: RF2, b&h: RF4, c&i: RF5, d&j: VMF2, e&k: VMF3, f&l: BF1.



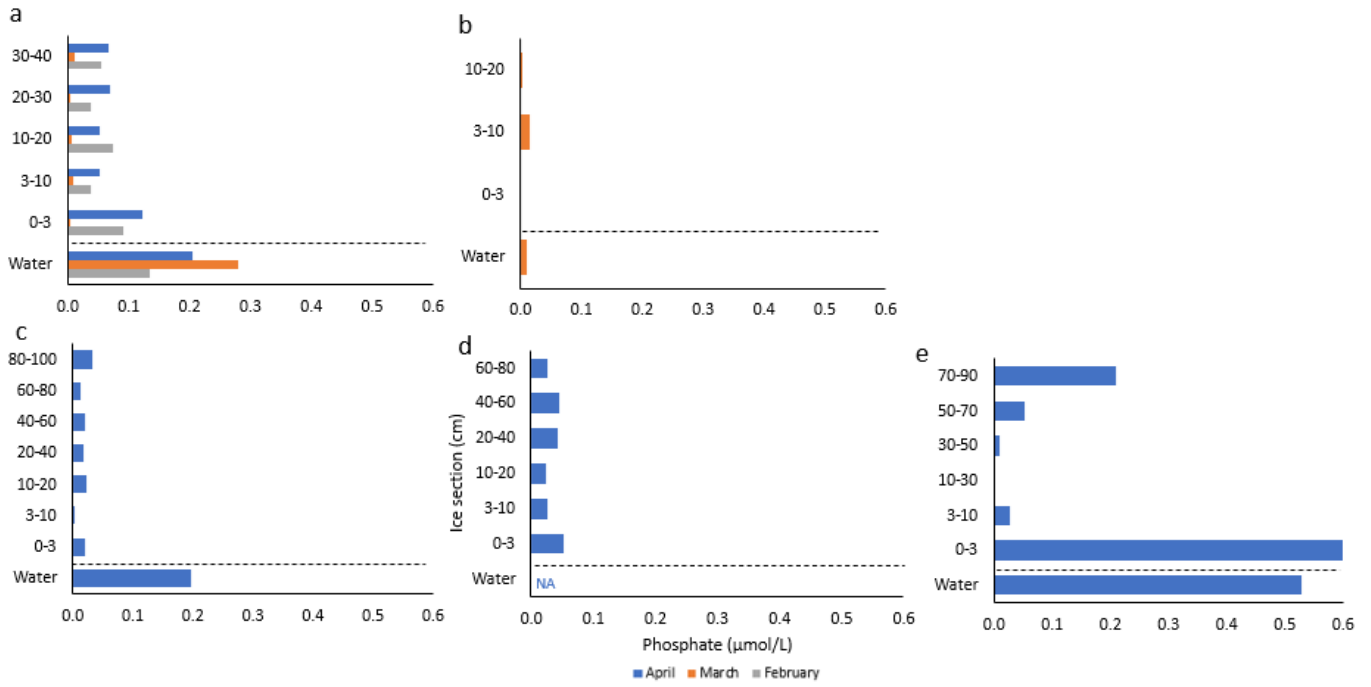
Appendix B. Vertical gradients of ice bulk salinity (left) and calculated brine volume fraction (right). a&g: RF2, b&h: RF4, c&i: RF5, d&j: VMF2, e&k: VMF3, f&l: BF1.



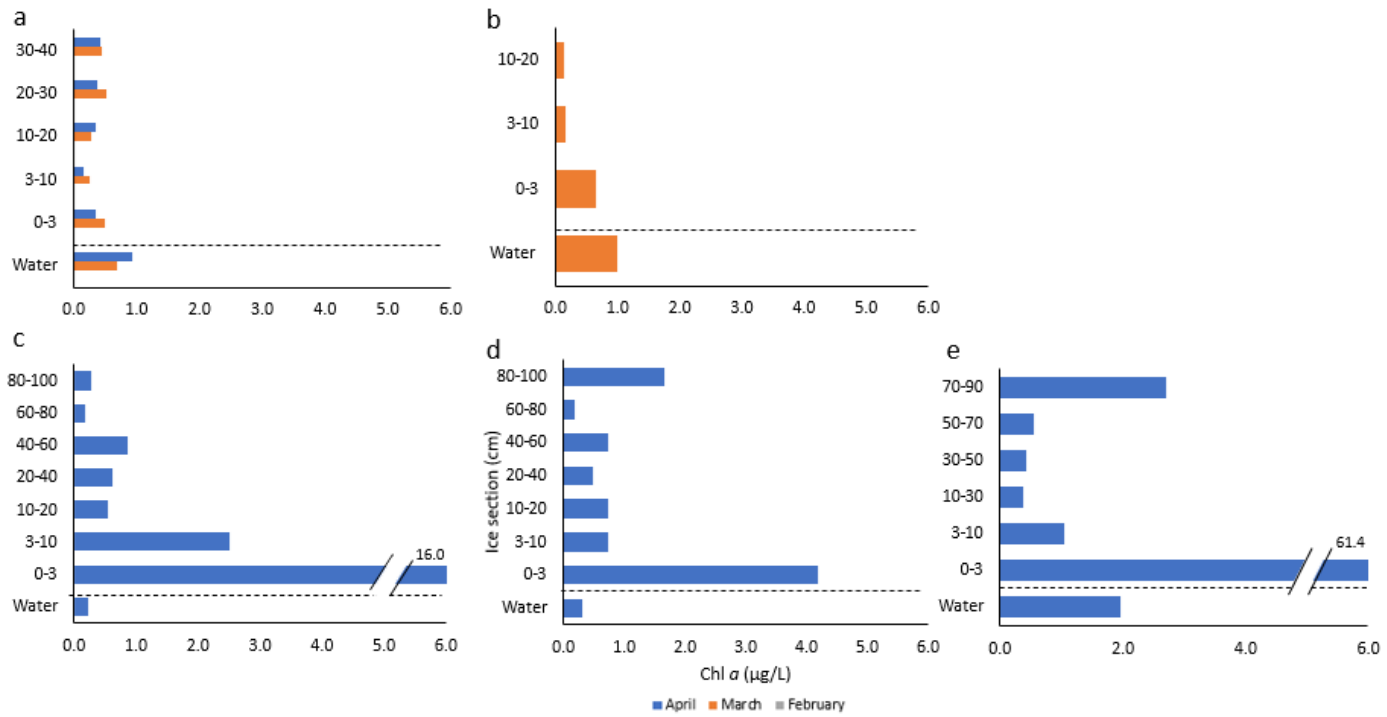
Appendix C. Silicate concentration in the water column and in the ice core sections. a: RF2, b: RF4, c: VMF2, d: VMF3, e: BF1.



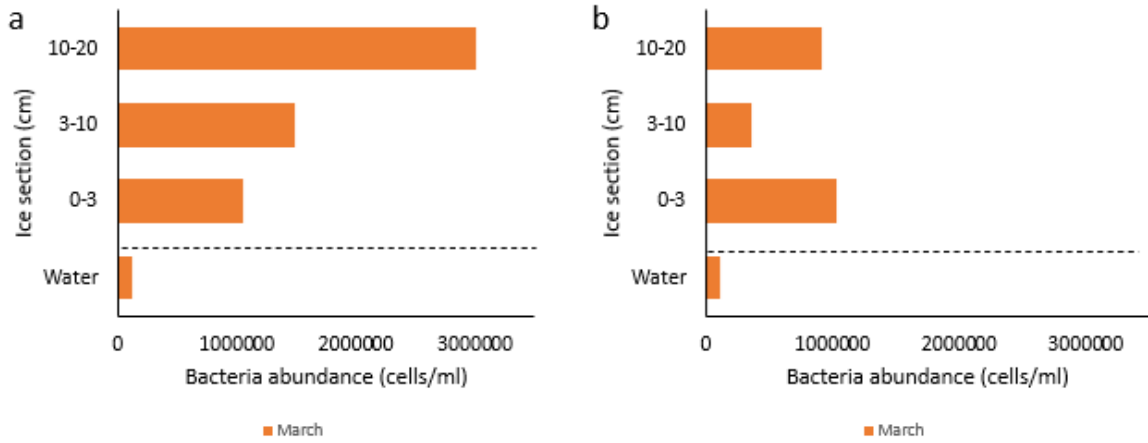
Appendix D. Nitrate concentrations in the water column and in the ice core sections. a: RF2, b: RF4, c: VMF2, d: VMF3, e: BF1.



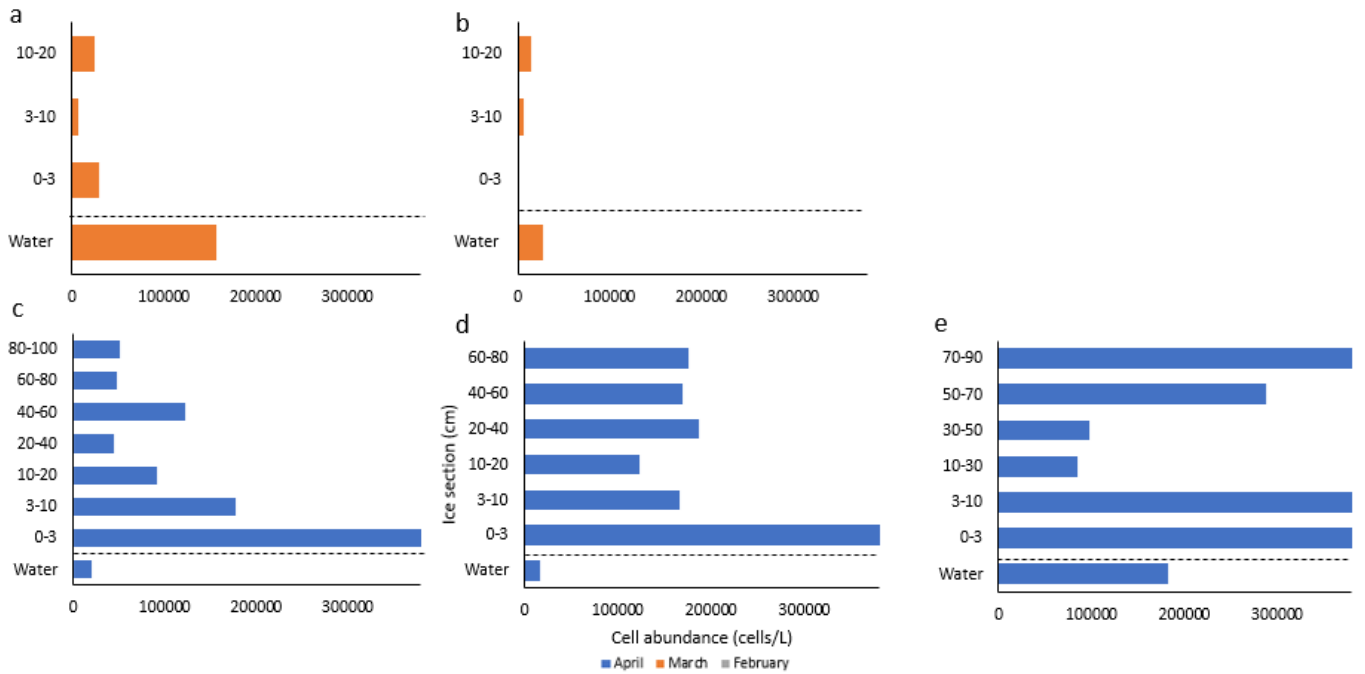
Appendix E. Phosphate concentrations in the water column and in the ice core sections. a: RF2, b: RF4, c: VMF2, d: VMF3, e: BF1.



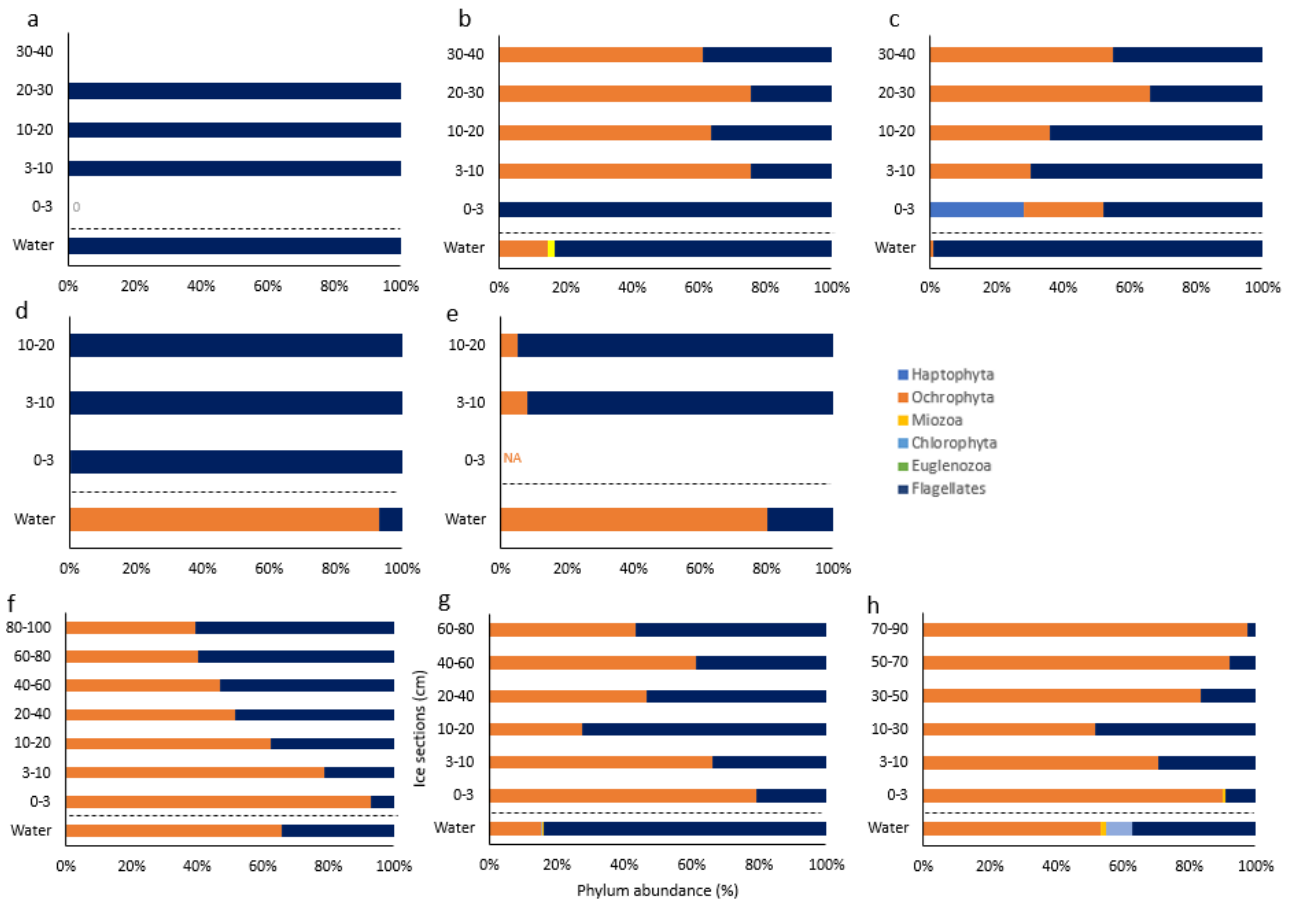
Appendix F. Chl a concentrations in the water column and in the ice core sections. a: RF2, b: RF4, c: VMF2, d: VMF3, e: BF2.



Appendix G. Bacteria abundance in the water column and in the ice core sections. a: RF4, b: RF5.



Appendix H. Cell abundance in the water column and in the ice core sections. a: RF4, b: RF5, c: VMF2, d: VMF3, e: BF2.



Appendix I. Relative contribution of different phyla to the algal composition in Ramfjorden, Van Mijenfjorden, and Billefjorden. a: RF2, February, b: RF2, March, c: RF2, April, d: RF4, e: RF5, f: VMF2, g: VMF3, h: BF2.

Appendix J. Basic light availability calculations for the sampled stations. Attenuation coefficients were retrieved from Zhang et al. (1999).

Station	Month	Snow (m)	Ice (m)	Attenuation snow (m ⁻¹)	Attenuation ice (m ⁻¹)	Assumed incoming light (%)	Assumed albedo	Under ice (%)
RF1	February	0.12	0.25	20	1.5	100	0.9	0.62
RF2	February	0.15	0.36	20	1.5	100	0.9	0.29
RF3	February	0.10	0.36	20	1.5	100	0.9	0.78
RF1	March	0.28	0.45	20	1.5	100	0.9	0.01
RF2	March	0.20	0.36	20	1.5	100	0.9	0.11
RF3	March	0.24	0.39	20	1.5	100	0.9	0.05
RF4	March	0.10	0.17	20	1.5	100	0.9	1.05
RF5	March	0.13	0.17	20	1.5	100	0.9	0.58
RF1	April	0.52	0.45	20	1.5	100	0.9	0.00
RF2	April	0.24	0.48	20	1.5	100	0.9	0.04
RF3	April	0.44	0.43	20	1.5	100	0.9	0.00
VMF1	April	0.08	0.75	20	1.5	100	0.9	0.66
VMF2	April	0.15	0.86	20	1.5	100	0.9	0.14
VMF3	April	0.13	0.83	20	1.5	100	0.9	0.21
BF1	April	0.06	0.92	20	1.5	100	0.9	0.76
BF2	April	0.10	0.79	20	1.5	100	0.9	0.41
BF3	April	0.03	1.28	20	1.5	100	0.9	0.80